Executive Summary

Sierra Geothermal Power Corporation's (SGP) Alum prospect is one of several promising geothermal properties located in the middle to upper Miocene (~11-5 Ma, or million years BP) Silver Peak-Lone Mountain metamorphic core complex (SPCC) of the Walker Lane structural belt in Esmeralda County, west-central Nevada. The geothermal system at Alum is wholly concealed; its upper reaches discovered in the late 1970s during a regional thermal-gradient drilling campaign. The prospect boasts several shallow thermal-gradient (TG) boreholes with TG >75^{o}C/km (and as high as 440^{o}C/km) over 200-m intervals in the depth range 0-600 m. Possibly boiling water encountered at 239 m depth in one of these boreholes returned chemical-geothermometry values in the range 150-230^{o}C. GeothermEx (2008) has estimated the electrical-generation capacity of the current Alum leasehold at 33 megawatts for 20 years; and the corresponding value for the broader thermal anomaly extending beyond the property at 73 megawatts for the same duration.

The SPCC, which in addition to Alum hosts the nearby Fish Lake and Silver Peak geothermal areas, accommodated initial slip transfer between major right-lateral strike-slip fault zones on opposite sides of the NW-trending Walker Lane. The core complex, hundreds of square kilometers in areal extent, consists of a ductiley deformed lower plate—mylonitized Proterozoic metasedimentary rocks and Cretaceous granitoid—separated from a lithologically diverse upper plate by a regional detachment-fault zone. The exposed upper plate at SGP's Silver Peak prospect, just south of Alum, is dominated by Proterozoic to Ordovician sedimentary rocks. By contrast, the upper plate at Alum, above the locally-designated Weepah detachment, consists principally of weakly consolidated siliciclastic sediments of the middle to upper Miocene Esmeralda Formation.

Older Esmeralda sediments at Alum, evidently deposited in an inaugural supradetachment basin of the SPCC, are mainly bouldery, polymict sedimentary breccias shed northwestward from the basin's inferred but now-erosionally-obliterated headwall breakaway fault. These early coarse clastics were moderately to tightly folded (probably in response to clockwise vertical-axis block rotation) and eroded prior to formation of a second, NNE-trending, listric-fault-bounded, half-graben basin to the northwest. The second basin was filled with tuffaceous siliciclastic sediments, comprising lacustrine muds to sands and fluvial pebble gravels, locally punctuated by low-volume felsic ash flows. A third, similarly-configured, listric-fault-bounded basin that formed northwest of the second is expressed in outcrop as tuffaceous mudstone to siltstone and coarse fluvial conglomerate.

The relict, supradetachment-basin-bounding, NNE-trending fault zones at Alum are ideally configured in the modern right-lateral-wrench-fault regime to be permeable structural aquifers for the active geothermal system. However, these faults are considered unlikely to be the system's "master" thermal-fluid conduits. Based on detailed geologic mapping, structural analysis, shallow-temperature data, and J. Witter's (2009, pers. comm.) SGP gravity modeling, the most plausible master-conduit candidates are inferred to be subregional, high-relief, normal- and normal-oblique-slip faults just north and west of and in the southeastern part of the property, as well as the Weepah detachment itself. The deeper the detachment within the prospect proper, the hotter, thicker, and more productive this portion of the geothermal reservoir is envisioned as likely to be.

Introduction

At the request of Sierra Geothermal Power Corporation (SGP), the writer has geologically mapped, in detail, and conceptually modeled the company's Alum geothermal prospect, in the western Weepah Hills of the Walker Lane structural belt in Esmeralda County, Nevada (Figures 1 and 2). Like SGP's Silver Peak prospect, just to the south (Figure 2), Alum is characterized by (**1**) anomalously high shallow thermal gradients; and (**2**) unusual structural complexity—features that in combination are auspicious for discovery of a commercial geothermal system at depth.

Aside from its geothermal potential, the Alum area is best known for being the site of a unique (for North America, at least), large deposit of hydrothermal potassium alum—$KAl(SO_4)_2$**.**$12H_2O$—with elemental sulfur. The deposit was discovered in 1868 (Spurr, 1906) and worked without success in 1921, 1939, and 1967 (?) (Albers and Stewart, 1972): It is now flourishing as a source of natural fertilizer, being mined by Heart of Nature LLC. The company holds (or has leased long-term) a 40-acre parcel of patented land that includes the mine.

GeothermEx (2008) has written a comprehensive geothermal-exploration history of the Alum property and vicinity, an account to which the reader is referred for the framework behind the following highlights. Prior geothermal exploration at Alum was conducted mostly by (or on behalf of) Amax Exploration, Inc., during the early 1980s, when the company completed numerous shallow to intermediate-depth thermal-gradient boreholes on the property. One of these holes, proximal to the Alum mine, (**1**) encountered hot (boiling?) water with a sulfurous aroma at 259 m (J.E. Deymonaz—formerly with Amax—pers. comm., 2008); (**2**) had an equilibrated (?) temperature of 105^{o}C at that depth; and (**3**) between the surface and 200 m boasted a thermal gradient of 440^{o}C/km. Numerous other holes on the property showed gradients in excess of 75^{o}C/km to depths ranging from 200 m to 600 m.

The property's geothermal potential was patent, and a deep (1830-2440 m) Alum exploration borehole had been planned when Amax terminated its geothermal endeavors in 1983. In that same year, the Amax Alum leases were dropped, and new, essentially co-located ones were issued to GeoEnergy Partners 1983, Ltd. (GEP). SGP acquired the bulk of these leases from GEP in 2005, and embarked upon the intermittent exploration program that encompasses the present study, and remains ongoing today.

Previous Work

The Alum property has been previously mapped geologically, but at smaller scales (1:62,500 and smaller; Albers and Stewart, 1972; Stewart, 1989; Diamond, 1990; Stewart and Diamond, 1990; Oldow et al., 2003) than mandated for the present specialized study. Stewart (1989), Diamond (1990), and Stewart and Diamond (1990) were the first to publish on the geology of the Alum area in the context of its location within a *bona fide* metamorphic core complex—since designated the Silver Peak-Lone Mountain complex (SPCC). In the Silver Peak Range, the first mountains west of the Weepah Hills, Elias (1995) determined that Neogene siliciclastic sedimentation atop the evolving core complex took place in northwestward-propagating, listric-fault-bounded, supradetachment half-graben basins.

The 1981-1983 Amax Alum exploration program was canceled before more than initial thermal-gradient drilling, fluid geothermometry (one sample); and preliminary logging of the retrieved borehole samples could be undertaken. More intensive exploration at Alum began in 2008, when SGP commissioned a gravity survey of the property and vicinity (including the Silver Peak prospect; Magee Geophysical Services, 2008). Fox (2008) interpreted results of that survey in the context of regional right-lateral wrench-fault tectonics: From this perspective, he suggested that a buried (and at the time undocumented) fault extending SSW from the Alum mine would be the property's most favorable geothermal target zone. SGP's Jeff Witter computer-modeled the gravity data to construct at least a dozen representative depth-to-bedrock profiles: Several of these were used to help constrain the detailed geologic sections offered in the present report.

GeothermEx (2008) completed a standard "43-101" independent technical report on the area, and estimated the electrical-generation capacity of the prospect and vicinity as set forth in the introduction to the current report.

Geologic Setting

(portions of this section are duplicated from Hulen, 2008)

Alum is one of two SGP "top-tier" geothermal prospects (the other being Silver Peak, about 10 km to the south) in the Walker Lane structural belt of west-central Nevada and east-central California (Figure 1***;*** Stewart and Diamond, 1990; Oldow et al., 2003; Wesnousky, 2005). The Walker Lane is a generally NW-trending transition zone separating the rigid Sierra Nevada block, on the west, from the essentially pure-extensional Basin-and-Range province on the east. Results from satellite-based space geodesy (Dixon et al., 2000) reveal that the Sierra Nevada block, or microplate, is moving NW, relative to a stable North America, at a velocity of about 14 mm/yr, while the Basin and Range is moving WNW at a much slower rate, only about 2-3 mm/yr (Oldow, 2003a). Between these two domains, the Walker Lane accommodates their velocity-vector differential by transtension, a type of strain in which, in this case, NW-directed right-lateral shear is accompanied by an element of WNW-oriented extension. This strain mode can be particularly amenable to the creation and maintenance of fracture porosity and permeability for geothermal-fluid flow and storage. Indeed, the largest active geothermal system in the United States—at the Salton Sea field in California (e.g., Elders et al., 1972; Hulen et al., 2002, 2003)—resides in a demonstrably transtensional tectonic regime.

The latitudinal range of the Walker Lane encompassing the Silver Peak and Alum prospects is characterized by eastward displacement transfer from major active right-lateral strike-slip fault zones in the western (to the south) and eastern (to the north) portions of the structural province (Oldow, 2003b; Oldow et al., 2003; Figure 1). The transfer is now accomplished by major left-lateral-oblique-slip faults of the Mina Deflection (Oldow et al., *op. cit.*; Figures 1 and 2), but between ~11 and 5 Ma the process was effected via the SPCC. Akin to other such structures throughout North America

(e.g., Davis and Lister, 1988), the SPCC is characterized by a broadly upwarped, locally-exposed, ductiley-deformed core—of mylonitized Proterozoic metamorphic rocks and Mesozoic granitoids—separated by a low-angle detachment-fault zone from overlying, stretched, complexly faulted and folded upper-plate formations ranging in age from Proterozoic through early Pliocene. Location of Alum and Silver Peak within the SPCC (Hulen, 2008) has important implications for the fundamental permeability architecture of both of these geothermal prospects.

Initial displacement transfer from the western to the eastern Walker Lane wrench faults (Figure 1) by the SPCC involved "dragging" of the upper plate northwestward above the ductile core (see drawings in Oldow, 2003b). The core, thus "unroofed," was forced to bulge upward as a means of restoring isostatic equilibrium. Elias (2005) deduced that profound upper-plate stretching resulted in formation of numerous, northwestward-propagating, supradetachment half-graben basins that were filled by Neogene siliciclastic sediments. In latest Miocene to early Pliocene time (~6 Ma [?] to ~5 Ma), according to Petronis et al. (2003, 2007), deeply-rooted, clockwise, vertical-axis rotation of the SPCC caused widespread folding of both the upper *and* lower plates, and apparently terminated active core-complex evolution. Since then, the "immobilized" SPCC has been broken (**1**) by right- and left-lateral-oblique-slip Walker Lane faults, the latter exemplified by those at the northern margin of the Silver Peak Range (Figure 2); and (**2**) by generally NNE-trending, moderate- to high-angle, normal- and oblique-slip faults systematically developed as subsidiary structures in the Walker Lane tectonic regime. The latter faults include the Paymaster Canyon fault at the eastern edge of Clayton Valley (Zampirro, 2003), and the historically active Emigrant Peak fault zone flanking eastern Fish Lake Valley (Reheis and Sawyer, 1997; Figure 2).

A portion of the Stewart and Diamond (1990) small-scale geologic map of the Alum area is reproduced (with color added) as Figure 3, which also shows the position of the Alum mine and the SGP leasehold in the western Weepah Hills. The writer's Alum geologic map agrees generally with—indeed, is broadly based upon—that of the earlier study, but departs substantially with respect to (**1**) the relative ages of Esmeralda-Formation units A

through F (adapted by Stewart and Diamond, 1990, from Moiola, 1969); (**2**) the origin and timing of locally tight folding of units E and F; and (**3**) the nature of the major fault at the western edge of the Figure 3 map area—a structure called the "NW corner fault (NFZ)" by GeothermEx (2008).

The newer work has also revealed a formerly undocumented, major normal-oblique-slip fault zone that bisects the leasehold from SSW to NNE; is probably a reactivated supradetachment-basin-bounding structure; and is exposed in the open pit of the Alum mine. This structure—herein designated the Alum fault zone, or AFZ—and the NFZ are spatially associated with intense hydrothermal alteration, and in all likelihood are major controls for modern-day thermal-fluid upflow. However, as discussed in detail later in this report, the principal sources of thermal fluid traversing these structures are believed to be subregional, deeply-penetrating, normal and oblique-slip faults a little west and north of the property.

Methods and Procedures

In the same approach utilized for the nearby Emigrant geothermal area and SGP's Silver Peak property (Figure 2; Hulen, 2008; Hulen et al., 2005a; 2005b), the Alum prospect and vicinity were geologically mapped, at a scale of 1:10,000 (1:10K), using mylar overlays on Digital-Orthophoto-Quadrangle panchromatic imagery (1-m resolution) mathematically fused with multispectral Advanced Spaceborne Thermal-Emission and Reflection Radiometer (ASTER) remote-sensing imagery (30-m resolution). Details of the data-fusion process and its advantages are discussed in Hulen et al. (2005b). The fused imagery, with no spherical aberration, effectively highlights rock types, structural trends, thermal features, and alteration that might otherwise escape detection. Eighteen individual 8 1/2 x 11" 1:10K geologic maps covering the prospect and surroundings are compiled as Appendix 1: The Alum mine area was too complex to be resolved even at 1:10K, and so was mapped at 1:6,000 (Appendix 2). The detailed mapping has been generalized into a 1:30,000 (1:30K)-scale map (Figures 4A and 4B), with corresponding geologic sections (Figures 5 through 8), for ease of reference and discussion. This

material provides the basis for the conceptual model of the prospect presented in the concluding section of the report.

Geology of the Alum Geothermal Prospect and Vicinity

Introduction

The 1:30K summary geologic map of the Alum prospect (Figure 4, with detailed explanation; see also Appendices 1 and 2) is broadly similar, for the same area, to the map of Stewart and Diamond (1990; Figure 3). However, the newer map shows significant structural departures of clear relevance to the prospect's geothermal potential. Discovery of these departures hinged upon recognition that the Esmeralda Formation (middle and upper Miocene) at Alum almost certainly accumulated and was deformed in a substantially different temporal sequence than initially interpreted by Stewart and Diamond (1990).

Lithology

Quaternary Surficial Deposits—Much of the Alum property, particularly the western half, is blanketed by Quaternary alluvium. This cover can be separated readily into older and younger accumulations, the first incised by the second. The older alluvium is extensively deflated to sparsely-vegetated and desert-varnished desert pavement.

Esmeralda Formation of the Eastern Part of the Leasehold—There is good evidence from the detailed mapping that Esmeralda Formation units E and F (Figure 3)—exposed over much of the eastern half of the leasehold and believed by Stewart and Diamond (1990) to be the youngest in the sequence—were actually the *oldest* Esmeralda units to be deposited here. Units E and F are described by Stewart and Diamond (1990) as consisting of a conglomerate facies (conglomerate, sedimentary breccia, and megabreccia ["monolithologic breccia"]) and a siltstone-sandstone facies (siltstone and sandstone with minor mudstone and conglomerate) (Figure 3). Based on clast lithologies, those authors determined that the conglomerate facies was derived from the east; the siltstone-sandstone facies from the west. Results of detailed mapping support this determination..

This mapping has also shown that units E and F consist predominantly of coarse, unsorted, angular-clast sedimentary breccias (lithologic types **SB**, **SBS**, and **MB**; Figure 4), distinct from the rounded-clast pebble to boulder conglomerates cropping out at the western edge of the map area (unit **CCG**). Clasts in the eastern breccias, mainly Paleozoic carbonate and chloritic siliciclastic rocks with lesser felsic- to intermediate-composition Tertiary volcanics—can reach truly impressive sizes; some, in **MB** megabreccia, are 100 m and more in diameter. The carbonate clasts are intact—although commonly "jigsaw-puzzle"-brecciated and rehealed—but many of the siliciclastic ones, especially in the megabreccias, are weathering-disaggregated to grayish-green and -olive, micaceous sand and pebble gravel.

The coarse sedimentary breccias of units E and F are locally interstratified with finer-grained siliciclastic strata, as in the vicinity of the Alum mine, where siltstones and fine-grained sandstones (**ST**) prevail; and in a whitish belt of outcrops dominated by tuffaceous siltstone and sandstone with thin sedimentary-breccia interbeds (**STb**, the light blue-colored unit of Figure 4) in the southeastern portion of the map area.

Unit **STb** is notable for hosting numerous small, interstratified mounds, stringers, and lenses of grayish-appearing, coarse-crystalline thinolitic tufa (Appendix 2). The precursor of this distinctive tufa type is the mineral ikaite ($CaCO_3.6H_2O$), a hydrous calcium carbonate stable only at low temperatures (0-25^oC?; Bischoff et al., 1992). Considering this temperature-stability constraint and the nature of the enclosing strata, the Alum-area thinolite is envisioned to have precipitated from carbonated cold springs at the margins of and beneath a lake or lakes occasionally inundated by volcanic-ash fallout as well as small-volume landslides and debris flows.

Local thin stringers of felsic vitric ignimbrite (**IG**) are sandwiched concordantly within the Alum-area **ST** siltstone-sandstone stratigraphic package (Figure 4). At the base of this ignimbrite, there typically occurs a laminated, "crinkly"-appearing, <1 m-thick zone either of intensely silicified siltstone or silty chert. In view of these observations, the

ignimbrite could be either a sill or a sublacustrine eruptive preceded by siliceous hot-spring exhalations.

The coarse sedimentary breccias and interstratified rocks of the eastern part of the leasehold—unlike the rest of the Esmeralda formation to the west—were moderately to tightly folded into a series of SE-plunging, WNW-trending anticlines and synclines, beds in the limbs of which are locally vertical. These structures are abruptly truncated at the AFZ, west of which the Esmeralda, although gently folded locally, is typically SE-tilted *en masse*.

Three points of evidence favor units E and F being older rather than younger members of the Esmeralda Formation: (**1**) E and F are strongly folded, unlike the rest of the formation here. It seems highly unlikely that this strong folding could have been accomplished in allegedly younger E and F strata without similarly affecting supposedly older units to the west. (**2**) Development of SPCC supradetachment basins in the nearby Silver Peak Range took place successively from southeast to northwest (Elias, 2005). A reversal of this trend in the Weepah Hills sector of the core complex is kinematically unlikely. (**3**) Folded unit-E strata in the vicinity of the Alum mine are eroded and unconformably overlain by a mixed siliciclastic unit (**MCL**; Figure 4) that is found nowhere west of the AFZ.

With respect to the Alum geothermal prospect, the real significance of the new temporal position of Esmeralda units E and F is this: The units have undergone much more intense deformation than the rest of the formation to the west, and the two structural domains thus defined are sharply separated by the AFZ, a structural break that is likely to be one of the property's principal permeability fairways.

Esmeralda Formation West of the Alum Fault Zone—Between the NFZ and the AFZ, the Esmeralda Formation at Alum is a conformable siliciclastic sequence comprising, from oldest to youngest:

(1) Commonly tuffaceous siltstone and fine-grained sandstone (**ST**; Figure 4). These lithologies are fissile to platy-weathering and generally whitish to buff in color. They are planar-laminated to -thin-bedded for the most part, and likely accumulated predominantly in a lacustrine depositional environment.

(2) Volcaniclastic pebble conglomerate (**CG**) interstratified with non-welded vitric-lithic felsic ash-flow tuff (**AFT**) as well as minor silty fallout tuff (**TS**) and volcanic-clast sedimentary breccia (**SBV**). Clasts in the conglomerate are typically subrounded to well-rounded, and are dominated by felsic volcanic rock with minor pumice. The tuff—Stewart and Diamond's (1990) tuff of Big Smoky Valley—is "punky"-textured, mainly pale pinkish-gray to greenish-gray, and contains abundant purplish-gray, flow-banded rhyolite clasts that form diagnostic desert pavement. The sedimentary breccia is notable for its isolated but large (up to 5 m) boulders of densely welded felsic ignimbrite.

(3) Tuffaceous mudstone and siltstone with minor local sandstone and conglomerate (**MDS**). The signal characteristic of this unit is its near-universal "popcorn" texture, a result of weathering in combination with a relatively high content of smectite-family swelling clay(s). The clay likely formed mostly by diagenetic alteration of original volcanic ash in the rock, but ancillary local hydrothermal alteration cannot be ruled out. The smectite is accompanied in most locations by conspicuous, clear and colorless, crystalline gypsum, much of the mineral occurring as "fishtail" twins. Like the smectite, the gypsum is probably diagenetic.

The Post-Esmeralda Fm. (Pliocene?) "Alum Unit"—Sediments west of the NFZ were designated by Stewart and Diamond (1990) as the "Alum unit," of uncertain age relative to the Esmeralda Formation. In the prospect area, the conspicuous part of this unit is a horizontal to randomly- but gently-dipping, pebble to boulder conglomerate (**CCG**) that, although generally semi-consolidated, is locally flinty due to hydrothermal silicification (Figure 4). Beneath the conglomerate is a commonly flat-lying, weakly consolidated,

whitish and gypsiferous, tuffaceous mudstone and siltstone (also designated **MDS**) little different in appearance from younger sediments flanking the AFZ to the southeast (Figure 4).

The "Alum unit" is almost certainly younger than (or perhaps than the rest of) the Esmeralda Formation, as the unit is (**1**) very weakly to nearly unconsolidated unless altered; (**2**) mostly horizontal to subhorizontal in configuration, unlike the tilted and folded Esmeralda strata to the southeast; and (**3**) downdropped to the west, along the AFZ, against more deformed and initially better consolidated rocks east of the fault zone. The significance of this assertion, if valid, is that the intense hydrothermal alteration affecting the Alum unit is a relatively young feature of the prospect.

The age of the Alum unit is conjectural, but based on lithologic similarities and stratigraphic position, it may be correlative with Elias's (2005) early Pliocene (i.e., ~5 Ma) Fish Lake Valley sequence in the northern Silver Peak Range.

Miocene or Younger Hydrothermal Breccia—Alum-sulfur mineralization at the Alum mine is localized within and around a lenticular body of middle Miocene or younger hydrothermal breccia disrupting folded and tilted Esmeralda Formation siliciclastics (Appendix 2—this particular breccia body is too small to be shown at 1:30K). The Alum-mine breccia consists of whitish, angular blocks—up to at least 1 m in diameter—of intensely silicified siltstone and sandstone. No rhyolite (as identified by Spurr, 1906) was observed in the breccia, but the writer's mine mapping was necessarily hasty (because of liability issues), and the igneous rock conceivably might have been overlooked. The siltstone-sandstone blocks in the hydrothermal breccia are separated and supported in a matrix variously of rock flour and hydrothermal open-space-filling minerals dominated by alum. A second, larger breccia body north of the Alum mine (Figure 4; Appendix 2) is texturally similar to the mine breccia but both its clasts and matrix are densely silicified.

The siltstones and sandstones that host the Alum-mine hydrothermal breccia are cut by (presumably) genetically related, complexly ramifying alum veinlets. These veinlets occupy pure dilational fractures with no evidence of crushing or granulation. The geometry and texture of the veinlets, along with the "jigsaw-puzzle" texture of the spatially associated breccia, suggest that both features formed in response to high-temperature hydrothermal overpressuring, typically involving (though not requiring) a magmatic heat source (Sillitoe, 1985).

Rocks beneath the Weepah Detachment—The lower plate of the SPCC is not exposed within or adjacent to the Alum leasehold (Figure 4), but crops out extensively to the east (Figure 3). These exposures provide clues to the possible subdetachment geology of the concealed Alum geothermal sysem.

According to Stewart and Diamond (1990), the exposed lower plate in the western Weepah hills consists of metamorphosed (actually mylonitized) Late Proterozoic to Cambrian sedimentary rocks and Mesozoic (actually Cretaceous) granitic rocks (Figure 3). The writer extended a salient of his detailed (1:10K) mapping to the upper plate-lower plate contact just northeast of the Alum leasehold (Figure 3; Appendix 1, image B5) to examine local lower-plate compositions and textures.

In this admittedly restricted example of the lower plate, the principal lithologies are mylonitic granitoid and carbonate (Appendix 1). The unmetamorphosed Cambro-Ordovician sedimentary rocks mapped in this vicinity by Stewart and Diamond (1990) (Figure 3) instead are Esmeralda-Formation megabreccia. The granitoid and carbonate rocks of the lower plate here are hard and brittle, and both would support networks of open fractures at depth along and perhaps beneath the Weepah detachment in the Alum geothermal system.

Structure

Structural disruption in the Alum prospect and vicinity can be attributed principally to Miocene and younger Walker Lane tectonism during and after the lifespan (~11-5 Ma) of the active SPCC. The principal structural elements of the prospect and its surroundings are as follows: (**1**) The SPCC in general; (**2**) The Weepah detachment, separating the upper and lower plates of the core complex; (**3**) folds and supradetachment-basin-bounding listric faults in the upper plate; and (**4**) inferred, post core-complex, normal- and normal-oblique-slip Walker Lane faults.

The SPCC—The core complex, in a regional sense, was discussed in the Geologic Setting section of this report. In terms of the Alum prospect, the Weepah Hills sector of the complex is unusual in that upper-plate, supradetachment-basin sediments here, including those of the Esmeralda Formation, are in extensive direct contact with the lower plate itself. The typical situation elsewhere in the complex is for these sediments and basins to surmount thick sequences of disrupted Paleozoic formations and earlier Tertiary volcanic rocks (for example, at the nearby Emigrant [Hulen et al., 2005a, 2005b] and Silver Peak [Hulen, 2008] prospects). At Alum, apparent paucity of these older rocks in the upper plate beneath the Mio-Pliocene sediments might imply either: (**1**) greater weathering and erosion of the older rocks prior to formation of the core complex; or (**2**) greater hyperextension of the upper plate, resulting locally in severe attenuation or even tectonic removal of the older rocks concomitant with formation of the overlying supradetachment basins: In this way, the younger rocks conceptually would be progressively "lowered down" to approach and contact the lower plate.

The Weepah Detachment—Within the Alum leasehold, the Weepah detachment is entirely concealed (Figures 3 and 4). Where the writer documented the structure in outcrop northeast of the property (Appendix 1, image B5), the detachment is a surprisingly subtle feature, apart from the fact, of course, that it separates disparate lithologic domains. Although the lower-plate rocks beneath the detachment here are intensely mylonitized, at the detachment itself there is a conspicuous lack of a thick and

potentially permeable cataclasite/fracture zone, like, for example, the ones described at this interface for the Silver Peak (Hulen, 2008) and Emigrant prospects (Hulen et al., 2005a; 2005b). One possible reason for this discrepancy is that upper plate rocks in the image B5 map area are weakly consolidated Esmeralda Formation sedimentary breccias (lithologic type **SBS**; Figure 4; Appendix 1). Movement of these (in bulk) non-brittle breccias might not have been conducive to formation of cataclasite and affililated fractures in the detachment zone.

Stewart and Diamond (1990) (Figure 3) mapped an extensive area of upper-plate Paleozoic carbonates and Tertiary volcanic rocks WSW of the leasehold. If these rocks are present at depth beneath the property, the detachment zone therein should be cataclastic and fractured. The Alum upper-plate carbonates themselves—as at Emigrant and Silver Peak—conceptually could harbor large volumes of thoroughly fractured, potential geothermal-reservoir rock.

The regional detachment of the SPCC—including the Weepah detachment—is "folded in doubly-plunging, northwest-trending folds with half-wavelengths of 5-10 km and amplitudes of 1-1.5 km" (Petronis et al., 2003; Oldow, 2003a). This folding is interpreted to have been effected by "shear-induced shortening of the lower-plate footwall"(Oldow, 2003a), which in turn would have induced clockwise vertical-axis block rotation—and consequent, fold-inducing compression—of both the upper *and* lower plates (Petronis et al., 2003).

Upper-Plate Folds at Alum—Theoretically, it seems likely that the weakly-consolidated, upper-plate Esmeralda Formation sediments at Alum would have been far more susceptible—in response to the above-noted block rotation—to deformation into classical anticlines and synclines than the crystalline and metasedimentary rocks of the lower plate. Field examination confirms this supposition. Nearby lower-plate exposures, east of the leasehold, occur as WNW-NW-trending "turtlebacks," erosionally belying their elliptically domal configuration (Stewart and Diamond, 1990; Oldow, 2003a). However,

although mylonitized, the lower plate rocks themselves are not obviously folded in alignment with the turtleback axes.

On the other hand, units E and F within and near the leasehold are strongly folded (Figure 4), and the axes of the folds—at least those east of the AFZ—mimic the turtleback trends. The 1-1.5 km half-wavelengths of the folds, as mapped by Stewart and Diamond (1990; their Figure 7), are less than a third of the corresponding regional parameter for the turtlebacks. This disparity suggests that although the turtlebacks and upper-plate folds developed contemporaneously, there was significantly more "crumpling" of the soft layered sediments of the Esmeralda Formation than of the massive crystalline rocks of the lower plate. The crumpling may have been accompanied, east of the Alum mine, by development of a small-scale overthrust fault, later mineralized with alum and sulfur.

As we have seen, folding of the Esmeralda Formation at Alum is dramatically more intense to the east of the AFZ than to the west of this structure (Figure 4). Stewart and Diamond (1990) portrayed this disparity (their Figure 7), but did not explain it. Prospect-wide detailed mapping and discovery of the AFZ provides the explanation: Esmeralda Formation units E and F were rotated clockwise, folded, perhaps locally thrust-faulted (about 800 m east of the Alum mine; Figure 4) and eroded prior to inception of this major fault zone.

The foregoing observations and relationships, if confirmed, have important implications for the tectonic history of the SPCC. Oldow (2003a) and Petronis et al. (2003) concluded that block rotation with folding took place as the culminating episode of core-complex evolution. Results of the present study, on the other hand, indicate that the bulk of the folding, and therefore block rotation and turtleback development, may have occurred before the younger Esmeralda sediments began to accumulate.

Upper-Plate, Supradetachment-Basin-Bounding Faults—The AFZ and NFZ are characterized in this report, for the first time, as the headwall breakaway faults of successive supradetachment basins in the evolving SPCC (Figures 4-8). The

corresponding (and requisite) fault zone for the initial supradetachment basin (the one receiving unit E and F sediments) has been erosionally removed.

> ***Note:*** Early 1980's lithologic logs for the Alum thermal-gradient boreholes (e.g., Figure 5; see also GeothermEx, 2008) were not utilized to constrain the current report's geologic sections. Based on the detailed geologic mapping, it is likely that borehole samples initially identified as being from *in situ* Paleozoic formations were actually from Esmeralda-Formation sedimentary breccias rich in Paleozoic-rock clasts

Both the AFZ and NFZ have highly braided traces (Figure 4), and both have prominent "scallops" in their footwalls. These configurations are consistent with normal- or normal-oblique faulting and westward "calving" of spoon-shaped subsidiary fault blocks due to headwall failure. Rare exposed slickensided surfaces along both fault zones range in dip from 46^{o} to 70^{o}, with two separate rake measurments of 60^{o} southward. The throws of these faults are conjectural, but can be estimated and inferred, respectively, from the results of gravity modeling and reasonable westward projections of the northwest-dipping Weepah detachment. Accordingly, both the AFZ and NFZ are suspected to have throws mostly in the 1-2 km range, and probably no more than 2.5 km.

Both of these fault zones are interpreted to dip progressively more gently with depth, ultimately to merge, listric-fashion, with the detachment (Figures 6 to 8). However, other configurations are permissible for these structures, as documented in an extensive detachment literature (e.g., Coney, 1980; Spencer, 1984; Spencer and Welty, 1986; Reynolds and Lister, 1987; Wilkins, Jr., et al., 1986; Davis and Lister, 1988): (**1**) The faults could dip, moderately or steeply, straight into the detachment, where the upper-plate structures could be abruptly truncated. (**2**) The AFZ and NFZ might be "domino-style" block faults. If so, the domino blocks likely would be more structurally complex (favoring higher fracture permeability) toward their bases—the complexity arising from "space problems" inherent in the blocks' formation and tectonic dispersal.

Two other normal- or normal-oblique-slip faults were mapped in the Alum area—one fault just northwest of the leasehold; the other just outside, then entering, the southwestern part of the property (Figure 4). These two structures appear to be of

minimal tectonic significance. A third, inferred fault just off the property's northeasternmost corner (Figure 4), is appropriately configured to be a strike-slip transfer structure at the northern end of the AFZ.

Post-Core-Complex High-Angle Faults—The most prominent high-angle faults in the vicinity of the Alum prospect are inferred from a detailed gravity survey of the area (Magee Geophysical Services, 2008) and subsequent computer modeling of the gravity data (J. Witter, pers. comm.., 2009), but for the most part are outside the 1:30K map area. These inferred major faults, apparently entirely concealed, essentially bound the northern western, and southwestern margins of the Weepah Hills. The structures may well turn out to be the parent thermal-fluid aquifers for the Alum geothermal system. Discussion of these potentially critical faults is therefore deferred for the concluding "Discussion and Conceptual Modeling" section of the present report.

Hydrothermal Alteration

Although most of the Mio-Pliocene siliciclastic sequence at Alum has been altered to a greater or lesser degree, only three areas are affected unambiguously by pervasive and intense hydrothermal alteration (Figures 4 and 9). Outside these areas, the widespread alteration—especially smectite alteration of gypsiferous mudstones and siltstones—is believed to be diagenetic, as such low-temperature "burial" alteration is typical of sediments initially rich in volcanic ash (Wohletz and Heiken, 1992).

Budgetary constraints precluded detailed instrumental mineralogic analysis for this project, but many of the secondary minerals occurring on the prospect were either megascopically identifiable or could be inferred based on extrapolation from outcrop samples earlier characterized petrographically by Pilkington (1983; Appendix 3). The principal hydrothermal phases thus identified for the project were quartz, chalcedony, opal, alum, sulfur, smectite, generic "clay," and pyrite or marcasite. The "clay" could be kaolinite, or a mixture of "clay-like" materials including alunite, allophone, or even microcrystalline zeolite: rigorous identification remains to be accomplished. Almost all

of the pyrite/marcasite, in the near-surface realm, has been oxidized to "limonite," comprising earthy to porcelaneous goethite, hematite, and jarosite (and probably other hydrous iron-bearing sulfates). The limonite imparts gaudy brownish-red, brownish-yellow and -orange, or golden hues to many of the property's most intensely altered outcrops.

The largest (~2 x 1.5 km) hydrothermal-alteration area on the property, along and adjacent to the AFZ in the vicinity of the Alum mine (Figure 9), is conspicuous for this showy coloration as well as brilliant-white patches in which the original character and mineralogy of the parent rock have been obscured to obliterated. Pilkington's (1983) petrographic samples A5, A8, and A10 (Figure 9; Appendix 3) were collected from this area, which we will call the Alum alteration domain. Sample A5 is ignimbrite that Pilkington describes as silicified and moderately welded (although the welding is not apparent under a 10X hand lens). Sample A8 is described as quartz-alunite rock "so strongly altered that none of the primary minerals can be identified"; accompanying secondary phases are "chalcedonic silica, kaolinite, and perhaps montmorillonite (i.e., smectite)." Sample A10 was identified as a clay-bearing chert conglomerate, but based on the mapping, the rock is probably silicified conglomerate or sedimentary breccia of unit **MCL** (Figures 4 and 9).

TG borehole 56-29 (Figure 9) is situated in the western and most intensely altered portion of the Alum alteration domain. Amax geological descriptions (from SGP electronic files) for this borehole note abundant, coarsely-crystalline pyrite in "white mylonite" below 200 m depth. The writer suspects that this "mylonite" is actually quartz-alunite-kaolinite-altered siliciclastic rock or cataclasite similar to sample A8, as described above.

Pilkington's (1983) petrographic descriptions, the 56-29 geologic log, and the local occurrence of hydrothermal alum and sulfur all point to the Alum alteration domain being mostly of the advanced argillic, or acid-sulfate, type (e.g., Hayba et al., 1985). This type of alteration is associated with low-pH hydrothermal conditions; and commonly with boiling hydrothermal fluids. Advanced argillic alteration develops in low-pH

hydrothermal systems both at relatively low (<<180^{o}C) and relatively high (250^{o}C to >300^{o}C) temperatures. The presence of chalcedonic silica in sample A10 suggests that the Alum-domain advanced argillic alteration is of the lower temperature type: Except under very unusual conditions, chalcedony forms and is stable in hydrothermal systems only at temperatures <~180^{o}C (Fournier, 1985).

Recall that, based on evidence presented in the previous section of this report, hydrothermal breccia found within and in the vicinity of the Alum mine is very likely of high-temperature hydrothermal origin (in the opinion of the writer, probably >250^{o}C). Therefore, the exposed, advanced argillic alteration of the Alum domain may have been effected during the waning stages of the causative hydrothermal system.

A second large (~1.3 x 0.6 km) hydrothermal-alteration patch on the Alum prospect occurs along the NFZ in and adjacent to the western part of the Alum leasehold (Figure 9). This alteration domain is dominated by massive silicification of "Alum unit" coarse conglomerate (**CCG**) and, to a lesser extent, of structurally juxtaposed ash-flow tuff and fine-grained siliciclastics. Associated secondary minerals are smectite (based on a "popcorn" weathering texture), gypsum, pyrite or marcasite (and their limonitic oxidation products), and an unknown whitish clay that could be kaolinite or a microcrystalline "clay-like" aggregate.

The western alteration patch at Alum is unique for the property in hosting silicified bladed calcite (although this material has only been found, in float, at a single site just below the NFZ). Silicified bladed calcite signifies precipitation of the carbonate from boiling hydrothermal fluid (Simmons and Christensen, 1994) followed by silicification of the mineral in response to boiling-induced fluid cooling.

The third and smallest Alum hydrothermal-alteration patch occurs within and proximal to the northeasternmost corner of the leasehold (Figure 9). This patch of alteration is bright white, and made up dominantly of clay (including some montmorillonite) and perhaps "clay-like" material with minor gypsum and limonite. The high albedo of the alteration,

in common with portions of the Alum alteration domain, suggests that the northern patch might also include microcrystalline alunite and kaolinite.

Note on Figure 9 that the two largest hydrothermal-alteration patches occur within the modern-day shallow temperature anomaly defined by the 54^{o}C isotherm @ 1200 meters elevation (GeothermEx, 2008). However, a relationship—if any beyond spatial—between the alteration and a modern geothermal system cannot be reliably established at this stage of the investigation.

Discussion and Conclusions; Conceptual Modeling

To set the stage for a conceptual model of the contemporary Alum geothermal system, Figure 10 is a generalized structure map of the leasehold and vicinity, showing major faults (mapped and inferred); exposed hydrothermal alteration; the modern shallow temperature anomaly; and the regional "ideal" fault system (from Christie-Blick and Biddle, 1985; and Sylvester, 1988) appropriate for this sector of the Walker Lane (Wesnousky, 2005). With this map and the corresponding geologic sections (Figures 4-8) as a framework, the essential components of the conceptual model—which can help to reduce the risks and costs of exploration and development—are as follows: (**1**) type and thermal vigor of the heat source; (**2**) nature and extent of permeability controls for thermal-fluid flow and storage; (**3**) sources and physical/chemical characteristics of the fluids; and (**4**) fluid-migration characteristics and patterns. Each of these components is discussed briefly in the following text, some of which is extracted directly from a companion report for the Silver Peak prospect by Hulen (2008).

There is no evidence of a viable, still-cooling igneous heat source for the Alum geothermal system. The youngest known igneous manifestation in the area is at "The Crater," a basaltic cinder-cone/flow complex several kilometers south of the map area of Figure 10. Basalt from one of The Crater's flows was $^{40}Ar/^{39}Ar$ age-dated, for J. Witter (pers. comm.., 2009), at ~400,000 years. Even much younger basalts are typically sourced by low-volume dikes or dike swarms that (relatively speaking) cool quickly to

ambient temperatures and are uncommon as heat sources for continental geothermal systems.

For the present, it seems prudent to assume that the Alum prospect's geothermal fluids are heated in response to deep circulation in fractured rocks within a domain of thin continental crust and elevated regional heat flow (e.g., Blackwell, 1983; Forster et al., 1997; Wisian et al., 1999). The estimated regional "background" heat flow of 100-200 mW/m^2 for the SPCC and vicinity is amenable to the creation of "deep-circulation" geothermal systems. At a thermal gradient here of, say, 50^oC/km—assuming an average annual surface ambient temperature of 15^oC—deeply-circulating waters could be heated to 150^oC at a depth of 2.6 km.

The ultimate source of groundwater for the Alum geothermal system will have been rain- and snowfall on area uplands. However, Flynn and Buchanan (1993) have shown, using hydrogen- and oxygen-isotope geochemistry, that waters from active geothermal systems in the Basin and Range and Walker Lane are almost certainly of Late Pleistocene age (30,000-10,000 years ago), having accumulated beneath large pluvial lakes when the climate was much colder and wetter than it is today. This being the case, the most likely proximal source of thermal fluids for the Alum geothermal system will be Pleistocene waters stored deep within and beneath the basin fill of Big Smoky Valley (Figure 2).

It has been noted that the one thermal-fluid sample collected from previous drilling efforts at Alum has chemical-geothermometer temperatures ranging from ~150^oC to ~230^oC: This is certainly encouraging for the subsurface presence here of commercially viable geothermal-reservoir temperatures. However, a much more extensive fluid-sampling program is clearly warranted during the next phase of Alum exploration drilling.

Likely key structural controls for thermal-fluid flow in the Alum geothermal system are portrayed on Figure 10. Within the Alum leasehold itself, the principal upper-plate structural conduits will be the AFZ and NFZ, which—having originated as

supradetachment-basin-bounding faults—are by coincidence now ideally configured in the modern right-lateral wrench-fault regime to be optimally permeable fluid channels. Deeper fluid flow within the leasehold should occur along the Weepah detachment. However, based on reasonable projections to depth from outside the property—and considering the 1-1.5 km amplitudes of the regional "turtlebacks"—the detachment and the faults that sole into it (the NFZ and AFZ) are believed unlikely to occur on the property deeper than, say, 2-2.5 km. In view of the postulated 2.6 km depth to reach 150^{o}C, it seems likely that more deeply penetrating faults proximal to the leasehold are required for fluids of the requisite temperatures to have approached and entered the property: Parallel reasoning, based on configuration of the shallow temperature anomaly, was advanced by GeothermEx (2008).

Plausible candidates for the "master" faults feeding the Alum system are inferred from more than a dozen gravity-modeled "depth-to-bedrock" profiles computed by J. Witter (pers. comm., 2009). Based upon the buried, high-relief bedrock scarps thus revealed, the inferred master faults are situated just north, just west, and within and proximal to the southern part of the property (Figure 10; hachured bands). The northernmost scarp, considering inevitable "real-world" structural complexities, is comfortably close to the "ideal" trend for left-lateral, or R' strike-slip faults in the modern Walker Lane tectonic regime. Many such faults, but of left-oblique slip (with a down-to-the-north dip-slip component), occur in the northernmost Silver Peak Range at the southern margin of Big Smoky Valley (Figure 2).

The westernmost gravity-modeled buried-bedrock scarp, just off the Alum property, is northerly-trending and quite close to the optimally permeable "N" normal-oblique fault trend (Figure 10). On this basis, the "western-scarp" fault at Alum is perhaps the most likely of the three gravity-inferred major faults to dominate thermal-fluid upflow and input for the Alum geothermal system.

The southern buried-bedrock scarp has a modeled trace more erratic than those of the other two major structures. This trace consists of WNW-trending segments separated by

a NW-trending one, from the western end of which an offshoot scarp extends NNE—subparallel to the AFZ—about 1.5 km into the leasehold (Figure 10). Note that the WNW-trending segments of the southern structure mimic the "ideal" right-lateral P-shear orientation (although here as for the inferred major fault north of the property, there clearly must be a considerable component of dip slip). If the WNW-trending segments are, in fact, modified right-lateral-oblique P shears, then the intervening NW-trending segment could be a releasing bend (e.g., Christie-Blick and Biddle, 1985), highly favorable for dilatancy and for fracture-permeability creation and/or enhancement.

Based on the foregoing concepts and logic, Figure 11 presents a graphical, NW-SE-oriented conceptual model of the active Alum geothermal system. According to the model, thermal fluids heated by deep circulation within and beneath Big Smoky Valley coalesce into focused, relatively high-volume upflows along a deeply-penetrating left-lateral-oblique fault zone at the valley's southern margin. Some of the heated fluids advect back out into sub-basinal sediments at shallower elevations. The bulk of thermal-fluid advection, however, is deflected at depth southeastward along the Weepah detachment, thence upward along listric normal-oblique faults in the upper plate of the core complex. In essence, existing thermal-gradient boreholes on and near the Alum prospect tap a moderate-temperature outflow plume. The plume is mostly confined beneath incompetent, sparingly permeable, tuffaceous and clay-rich, fine-grained Mio-Pliocene siliciclastics.

Which brings us to this point: Any reasonable model for the Alum geothermal system must take into account the fact that the upper-plate Mio-Pliocene siliciclastics are typically only weakly to moderately consolidated, commonly very fine-grained (or with very fine-grained argillaceous matrix material like the sedimentary breccias) and regionally clay-altered by burial diagenesis. In other words, these sediments under normal circumstances should be incompetent aquicludes. However, within the two largest hydrothermal-alteration patches on the prospect (Figure 10), these sediments are commonly silicified and flinty-textured; similar alteration is not unlikely at depth: Whether or not this silicification is genetically related to the active geothermal system, it

certainly will have "prepared the ground" for the system by extensively embrittling sediments that otherwise would not have supported the creation and maintenance of fracture permeability.

References

Albers, J.P., and Stewart, J.H., 1972, Geology and mineral deposits of Esmeralda County, Nevada: *Nevada Bureau of Mines and Geology*, Bulletin 78, 80 p.

Bischoff, J.L., Fitzpatrick, J.A., and Rosenbauer, R.J., 1992, the solubility and stabilization of ikaite ($CaCO_3.6H_2O$) from 0^oC to 25^oC: *Journal of Geology*, v. 101, p. 21-33.

Blackwell, D.D., 1983, Heat flow in the northern Basin and Range province, *in* The role of heat in the development of energy and mineral resources in the northern Basin and Range province (anonymous editor): *Geothermal Resources Council*, Special Report 13, p. 81-92.

Christie-Blick, N., and Biddle, K.T., 1985, Deformation and basin formation along strike-slip faults, *in* Strike-slip deformation, basin formation, and sedimentation (K.T. Biddle and N. Christie-Blick, editors): *Society of Economic Paleontologists and Mineralogists*, Special Publication 37, p. 1-34.

Coney, P.J., 1980, Cordilleran metamorphic core complexes—An overview: *Geological Society of America*, Memoir 153, p. 7-31.

Davis, G.A., and Lister, G.S., 1988, Detachment faulting in continental extension—Perspectives from the southwestern U.S. cordillera: *Geological Society of America*, Special Paper 218, p. 133-159.

Diamond, D.S., 1990, Structural and sedimentological evolution of an extensional orogen, Silver Peak Range and adjacent areas, west-central Nevada: *University of California* at Los Angeles, Ph.D. Dissertation, 360 p.

Dixon, T.H., Miller, M., Farina, F., Wang, H., and Johnson, D., 2000, Present-day motion of the Sierra Nevada block and some tectonic implications for the Basin-Range province, North American cordillera: *Tectonics*, v. 19, p. 1-24.

Elders, W.A., Rex, R.W., Meidav, T., Robinson, P.T., and Biehler, S., 1972, Crustal spreading in southern California: *Science*, v. 178, p. 15-24.

Elias, E.A., 2005, Structural control of late Miocene to Pliocene volcanic and volcaniclastic deposition during upper-plate fragmentation in the Silver Peak extensional complex, west-central Great Basin: *University of Idaho* at Moscow, M.Sc. Thesis, 68 p.

Fournier, R.O., 1985, The behavior of silica in hydrothermal systems, *in* Geology and geochemistry of epithermal deposits (B.R. Berger and P.M. Bethke, editors): *Society of Economic Geologists*, Reviews in Economic Geology, v. 2, p. 45-62.

Flynn, T., and Buchanan, P.K., 1993, Pleistocene origin of geothermal fluids in the Great Basin, western United States: *Resource Geology*, v. 16, p. 60-68.

Forster, C.B., Caine, J.S., Schulz, S., and Nielson, D.L., 1997, Fault zone architecture and fluid flow—An example from Dixie Valley, Nevada: *Stanford University*, 21st Workshop on Geothermal Reservoir Engineering, Proceedings, 8 p. paper.

Fox, R.C., 2008, Interpretation of a gravity survey of the Alum and Silver Peak areas, Esmeralda County, Nevada: Consulting Report for Sierra Geothermal Power Corporation.

GeothermEx, Inc. ("**GTX**"), 2008, Independent technical report—Resource evaluation of the Alum geothermal project, Esmeralda County, Nevada: "43-101" Report for Sierra Geothermal Power Corporation.

Hayba, D.O., Bethke, P.M., Heald, P., and Foley, N.K., 1985, Geologic, mineralogic, and geochemical characteristics of volcanic-hosted epithermal precious-metal deposits, *in* Geology and geochemistry of epithermal deposits (B.R. Berger and P.M. Bethke, editors): *Society of Economic Geologists*, Reviews in Economic Geology, v. 2, p. 129-168.

Hulen, J.B., 2008, Geology and conceptual modeling of the Silver Peak geothermal prospect, Esmeralda County, Nevada: Consulting Report for Sierra Geothermal Power Corporation, 23 p.

Hulen, J.B., Kaspereit, D., Norton, D.L., Osborn, W., and Pulka, F.S., 2002, Refined conceptual modeling and a new resource estimate for the Salton Sea geothermal field, Imperial Valley, California: *Geothermal Resources Council*, Transactions, v. 26, p. 29-36.

Hulen, J.B., Norton, D.L., Kaspereit, D., Murray, L., van de Putte, T., and Wright, M., 2003, Geology and a working conceptual model of the Obsidian Butte (Unit 6) sector of the Salton Sea geothermal field, California: *Geothermal Resources Council*, Transactions, v. 27, p. 227-240.

Hulen, J.B., Nash, G.D., Deymonaz, J., and Schriener, A., 2005a, Hot prospect—DOE enables the Emigrant geothermal exploration and slimhole drilling project in Fish Lake Valley, Nevada: *Geothermal Resources Council*, Bulletin, v. 34, p. 176-183.

Hulen, J.B., Nash, G.D., and Deymonaz, J., 2005b, Geology of the Emigrant geothermal prospect, Esmeralda County, Nevada: *Geothermal Resources Council*, Transactions, v. 29, 22 p.

Magee Geophysical Services, LLC, 2008, Gravity survey of the Alum and Silver Peak prospects, Esmeralda County, Nevada: Consulting Report for Sierra Geothermal Power Corporation.

Moiola, R.J., 1969, Late Cenozoic geology of the northern Silver Peak region, Esmeralda County, Nevada: University of California at Berkeley, Ph.D. Dissertation, 139 p.

Oldow, J.S., 2003a, Active transtensional boundary zone between the western Great Basin and Sierra Nevada block, western U.S. cordillera: *Geology*, v. 31, p. 1033-1036.

Oldow, J.S., 2003b, Late Cenozoic displacement partitioning in the northwestern Great Basin, *in* Regional geology and gold deposits of the Silver Peak area, Nevada (H.G. Brown, editor): *Geological Society of Nevada*, 2003 Fall Field Trip Guidebook, Special Publication 38, p. 113-152.

Oldow, J.S., Kohler, G., and Donelick, R.A., 2003, Late Cenozoic extensional transfer in the Walker Lane strike-slip belt, Nevada, *in* Regional geology and gold deposits of the Silver Peak area, Nevada (H.G. Brown, editor): *Geological Society of Nevada*, 2003 Fall Field Trip Guidebook, Special Publication 38, p. 153-161.

Petronis, M.S., Geismann, J.W., Oldow, J.S., and McIntosh, W.C., 2003, Paleomagnetic and $^{40}Ar/^{39}Ar$ geochronologic data bearing on the structural evolution of the Silver Peak extensional complex, west-central Nevada, *in* Regional geology and gold deposits of the Silver Peak area, Nevada (H.G. Brown, editor): *Geological Society of Nevada*, 2003 Fall Field Trip Guidebook, Special Publication 38, p. 177-211 (Reprinted with permission from the *Geological Society of America*, Bulletin, v. 114, p. 1108-1130).

Petronis, M.S., Geismann, J.W., Oldow, J.S., and McIntosh, W.C., 2007, Tectonism of the southern Silver Peak Range—Paleomagnetic and geochronologic data bearing on the Neogene development of a regional extensional complex, central Walker Lane, Nevada, *in* Exhumation associated with continental strike-slip fault systems (A.B. Till, S.M. Roeske, J.C. Sample, and D.A. Foster, editors): *Geological Society of America*, Special Paper 434, p. 81-106.

Pilkington, H.D., 1983, Petrographic descriptions of selected surface rocks and core samples, Alum area, Nevada (4106A): *Amax Exploration, Inc.*, Interoffice Memorandum to J.E. Deymonaz, 6 p.

Reheis, M.C., and Sawyer, T.L., 1997, Late Cenozoic history and slip rates of the Fish Lake Valley, Emigrant Peak, and Deep Springs fault zones, Nevada and California: *Geological Society of America*, Bulletin, v. 109, p. 280-299.

Reynolds, S.J., and Lister, G.S., 1987, Structural aspects of fluid-rock interactions in detachment zones: *Geology*, v. 15, p. 362-366.

Sillitoe, R.H., 1985, Ore-related breccias in volcano-plutonic arcs: *Economic Geology*, v. 80, p. 1467-1514.

Simmons, S.F., and Christensen, B.W., 1994, Origins of calcite in the Broadlands-Ohaki geothermal system, New Zealand: *American Journal of Science*, v. 294, p. 361-400.

Spencer, J.E., 1984, Role of tectonic denudation in warping and uplift of low-angle normal faults: *Geology*, v. 12, p. 95-98.

Spencer, J.E., and Welty, J.W., 1986, Possible controls of base- and precious-metal mineralization associated with Tertiary detachment faults in the lower Colorado River trough, Arizona and California: *Geology*, v. 14, p. 195-198.

Spurr, J.E., 1906, Ore deposits of the Silver Peak quadrangle, Nevada: *U.S. Geological Survey*, Professional Paper 55.

Stewart, J.H., 1989, Description, stratigraphic sections, and maps of the middle and upper Miocene Esmeralda Formation in the Alum, Blanco mine, and Coaldale areas, Esmeralda County, Nevada: *U.S. Geologlcal Survey* Open-File Report 89-324, 33 p. and geologic map (1:62,500).

Stewart, J.H., and Diamond, D.S., 1990, Changing patterns of extensional tectonics—Overprinting of the basin of the middle and upper Miocene Esmeralda Formation in western Nevada by younger structural basins, *in* Basin and Range extensional tectonics near the latitude of Las Vegas, Nevada (B.P. Wernicke, editor): *Geological Society of America*, Memoir 176.

Sylvester, A.G., 1988, Strike-slip faults: *Geological Society of America*, Bulletin, v. 100, p. 1666-1703.

Wesnousky, S.G., 2005, Active faulting in the Walker Lane: *Tectonics, v. 24*, ms. TC3009, 35 p.

Wilkins, J., Jr., Beane, R.E., and Heidrick, T.L., 1986, Mineralization related to detachment faults—A model: *Arizona Geological Society Digest*, v. 16, p. 108-117.

Wisian, K.W., Blackwell, D.D., and Richards, M., 1999, Heat flow in the western United States and extensional geothermal systems: *Stanford University*, 24th Workshop on Geothermal Reservoir Engineering, Proceedings, 8 p. paper.

Wohletz, K., and Heiken, G., 1992, Volcanology and geothermal energy: Berkeley, *University of California Press*, 432 p.

Zampirro, D., 2003, Hydrogeology of Clayton Valley brine deposits, Esmeralda County, Nevada: *Nevada Bureau of Mines and Geology*, Special Publication 33, p. 271-280.

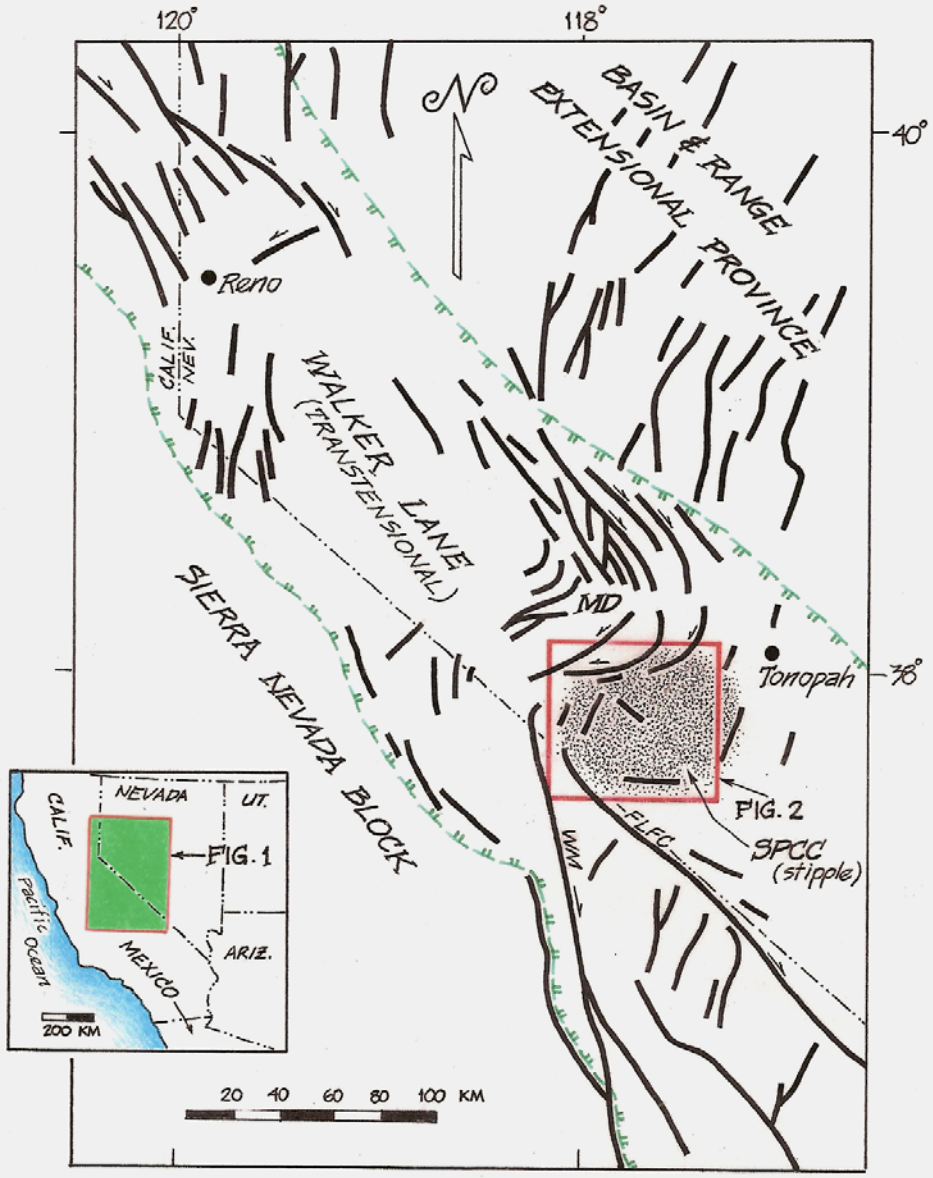

Figure 1. Late Cenozoic high-angle fault map of west-central Nevada and adjacent California, showing position of the Silver Peak-Lone Mountain metamorphic core complex (**SPCC**—stippled area), a recently active (i.e., geologically; through late Miocene at least) displacement-transfer feature, in the transtensional Walker Lane structural belt, in which the Alum and Silver Peak geothermal prospects are situated (see also Figure 2). Other abbreviations: **FLFC**—Fish Lake Valley/Furnace Creek fault zone; **MD**—Mina Deflection; **WM**—White Mountains fault zone. Please refer to text for additional explanation. Map minimally modified from *Oldow (2003b).*

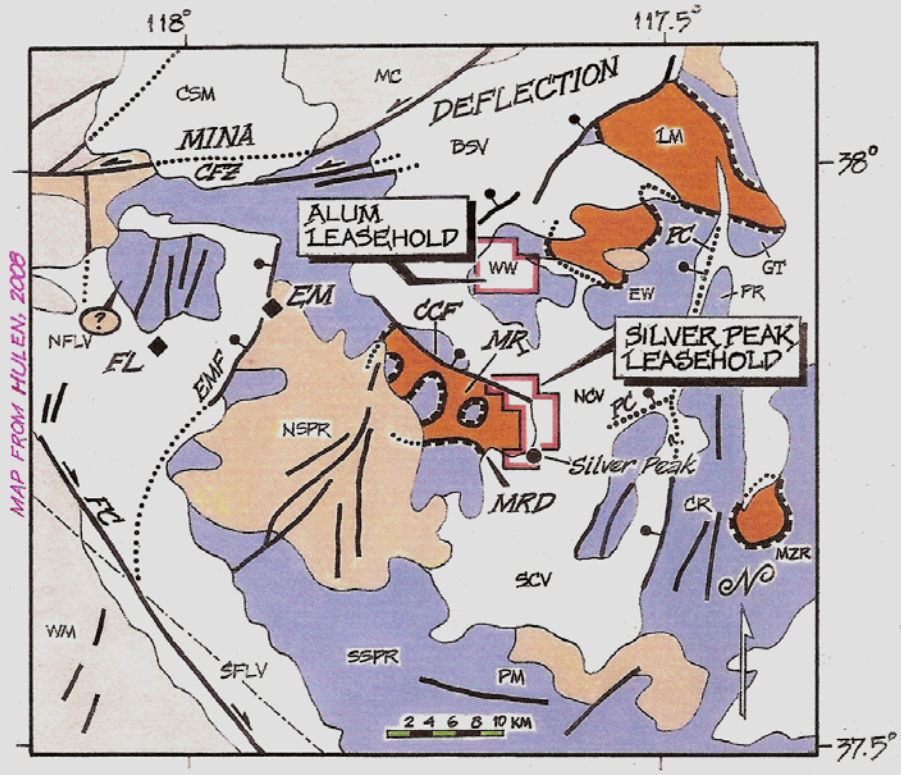

High-angle fault, bar-and-ball on downthrown block; half arrows showing lateral displacement; dotted where projected and concealed

Contact

Detachment fault, ornaments on upper plate; dotted where projected and concealed

◆ OR ▭ Geothermal prospect

Quaternary surficial deposits

Basement rocks, undivided

CORE COMPLEX

Post-detachment siliciclastic and volcanic rocks (Mio-Pliocene)

Sedimentary, volcanic, and intrusive rocks of the upper plate (Proterozoic to Miocene)

Extensively tectonized (mylonitized): Proterozoic metasedimentary rocks and Cretaceous granitoids of the lower plate, or "core"; broadly domed into northwest-trending "turtlebacks."

Figure 2. Highly generalized, small-scale geologic map of the Silver Peak-Lone Mountain metamorphic core complex, showing principal structures, lithologic packages, and geothermal prospects, including Alum (this report) and Silver Peak (Hulen, 2008). Map modified from Oldow et al. (2003b).

Abbreviations as follows: ***BSV***—Big Smoky Valley; ***CCF***—Cross-central fault; ***CFZ***—Coaldale fault zone; ***CR***—Clayton Ridge; ***CSM***—Columbus Salt Marsh; ***EM***—Emigrant geothermal prospect; ***EMF***—Emigrant Peak fault zone; ***EW***—eastern Weepah Hills; ***FC***—Furnace Creek fault zone; ***FL***—Fish Lake geothermal prospect; ***GT***—General Thomas Hills; ***LM***—Lone Mountain; ***MC***—Monte Cristo Range; ***MR***—Mineral Ridge; ***MRD***—Mineral Ridge detachment; ***MZR***—Montezuma Range; ***NCV***—northern Clayton Valley; ***NFLV***—northern Fish Lake Valley; ***NSPR***—northern Silver Peak Range; ***PC***—Paymaster Canyon fault (fr. *Zampirro, 2003)*; ***PM***—Palmetto Mountains; ***PR***—Paymaster Ridge; ***SCV***—southern Clayton Valley; ***SFLV***—southern Fish Lake Valley; ***SSPR***—southern Silver Peak Range; ***WM***—White Mountains; ***WW***—western Weepah Hills

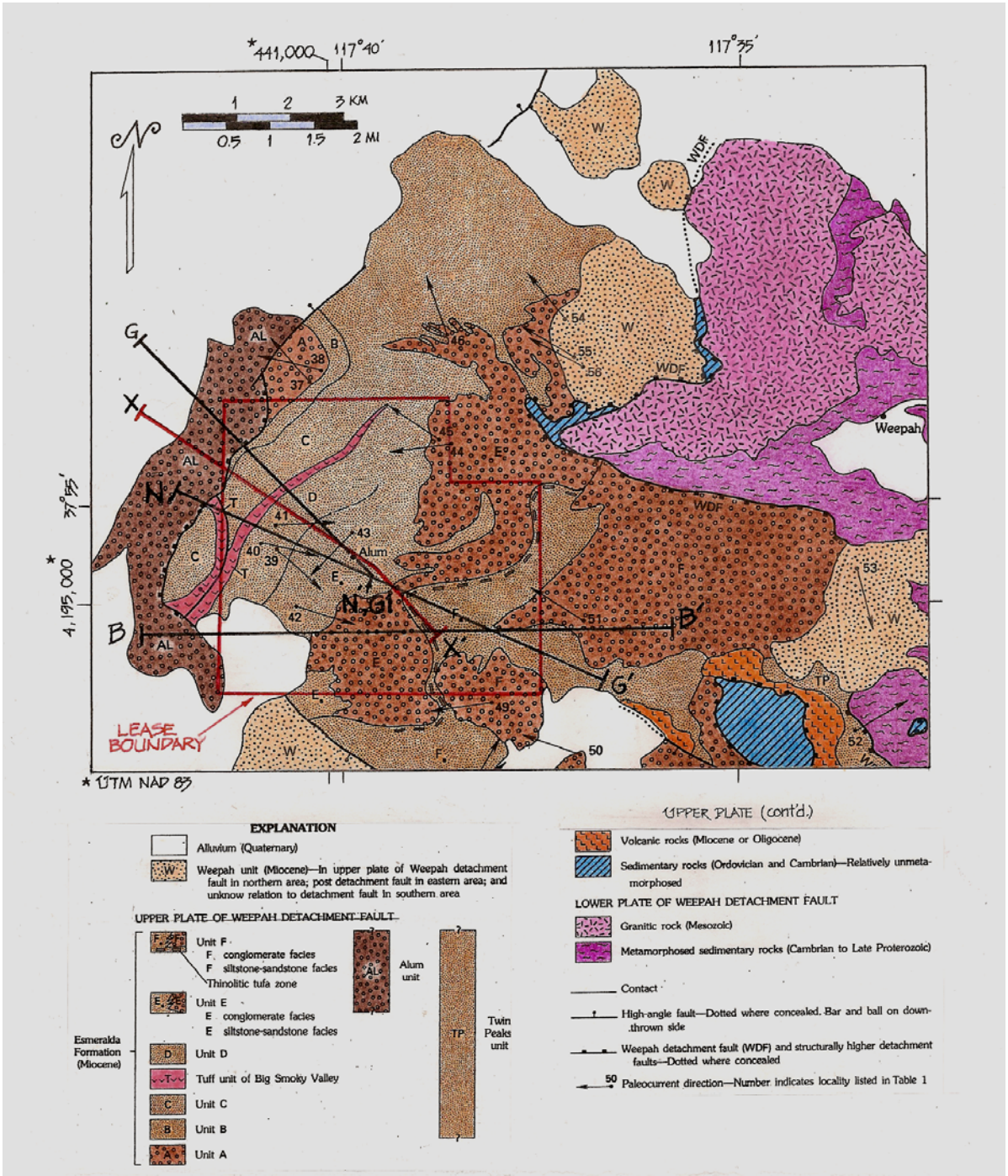

Figure 3. Stewart and Diamond's (1990) small-scale geologic map of the Alum area (Weepah Hills), with location of Sierra Geothermal's lease block (red outline) and positions of geologic sections (**B-B'**; **G-G1-G'**; **N-N'**; and **X-X'**) offered in the present report. Detailed mapping has revealed that the "detachment" at the western edge of this map area is actually a major, moderately to steeply west-dipping, normal-oblique fault that has focused hydrothermal fluid flow in the geologically recent past, and may continue to do so today.

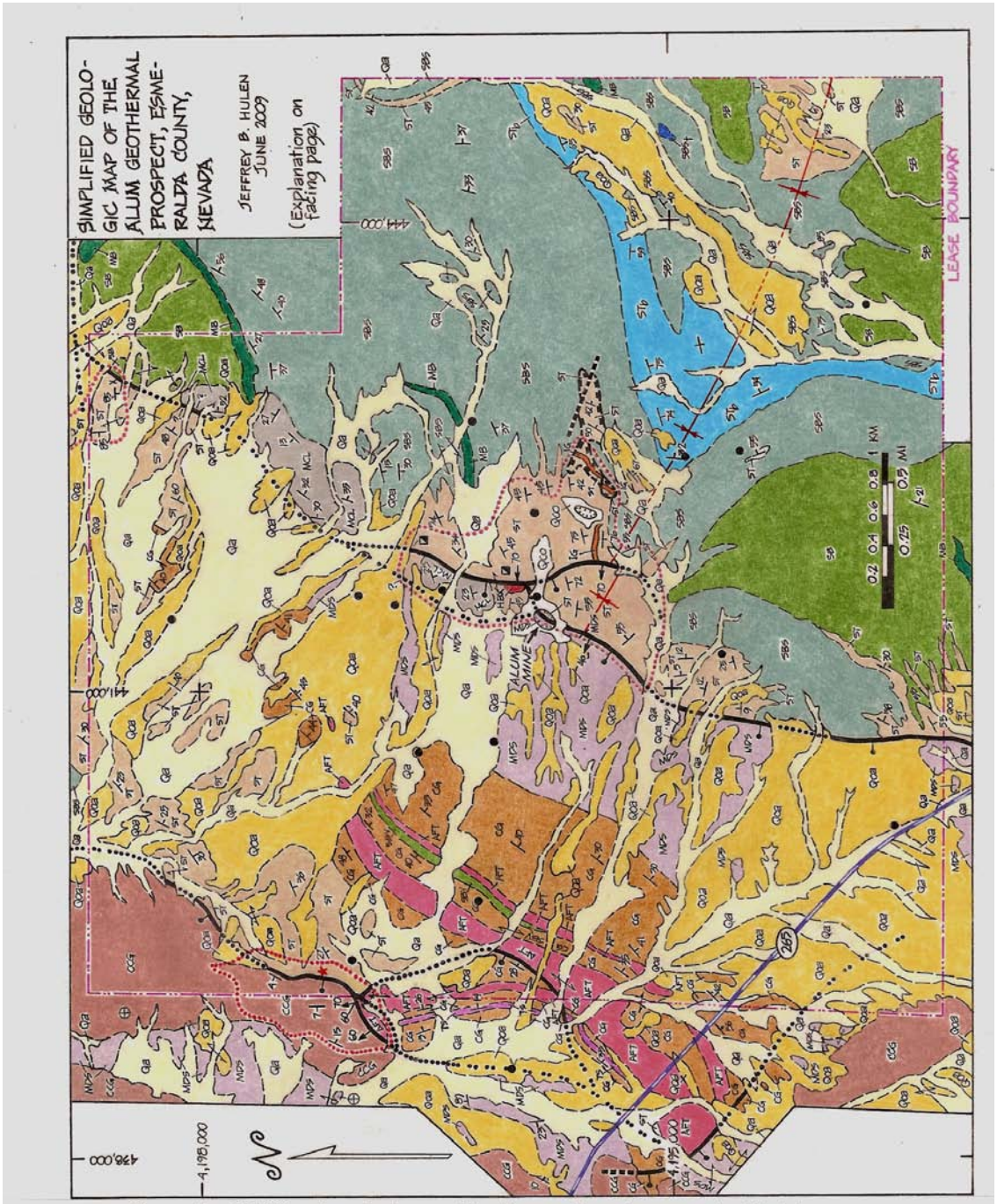

Figure 4A. 1:30,000-scale geologic map of the Alum geothermal prospect, simplified from 1:10,000 and 1:6,000-scale field sheets (see Appendices). Cross-section lines omitted for clarity (see Figure 4B).

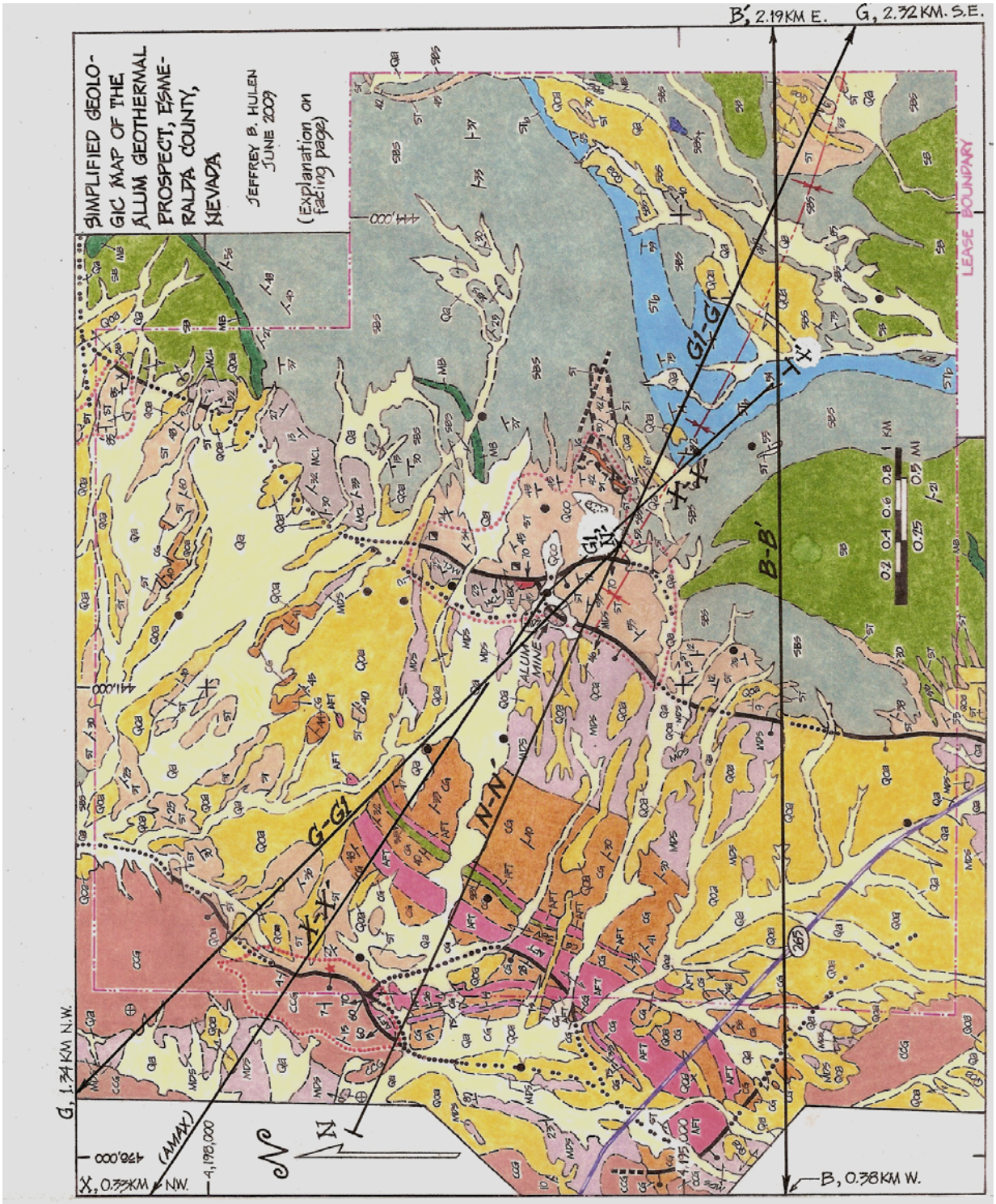

Figure 4B. Same map as Figure 4A, but with locations of geologic cross sections.

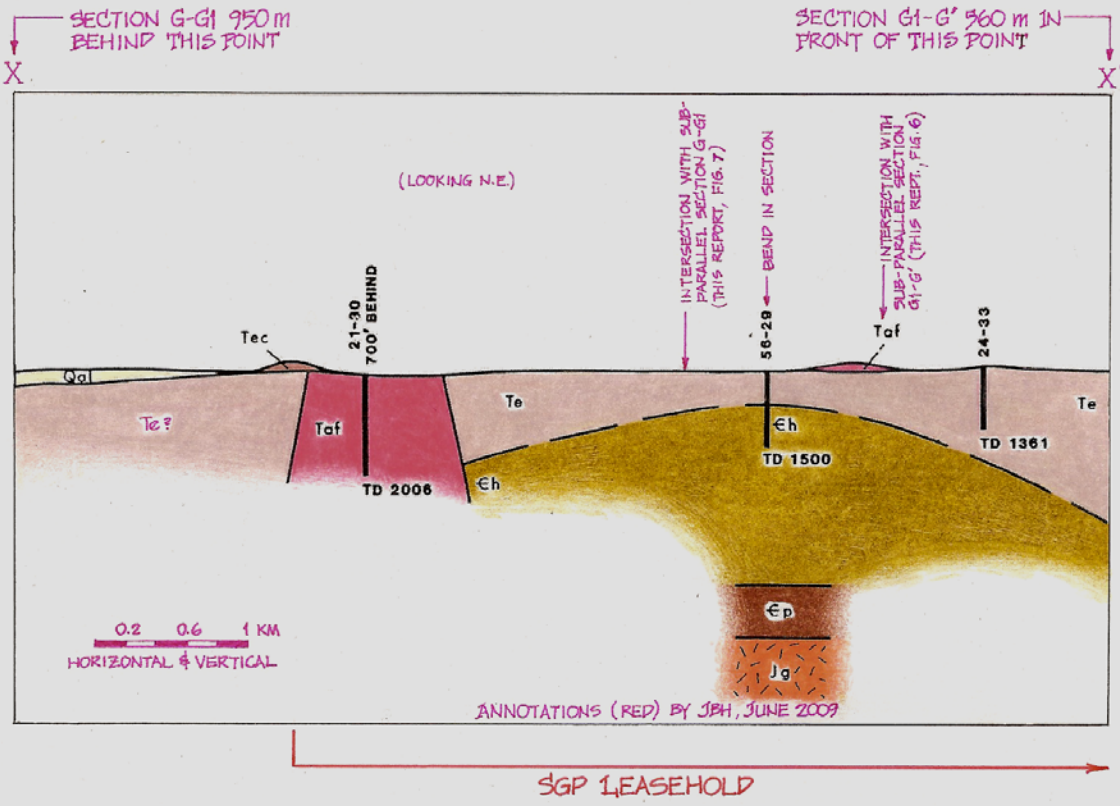

Figure 5. AMAX, Inc., interpretive, NW-SE-oriented geologic section **X-X'** (ca. 1982) through three of that company's Alum-prospect thermal-gradient boreholes (section retrieved from Sierra Geothermal Corporation electronic files; for location of section, see Figures 3 and 4B). No explanation, but the geologic units portrayed are almost certainly as follows: **Qal**—Quaternary alluvium; **Te**—Tertiary (Miocene) Esmeralda Formation, siltstone-sandstone facies; **Tec**—Esmeralda Formation, conglomerate facies; **Taf**—Tertiary (Miocene) ash-flow tuff; **Eh**—Cambrian Harkless Formation; **Ep**—Cambrian Poleta Formation; **Jg**—Jurassic granitoid. Compare this section with sub-parallel **G-G1-G'** of the present report (Figures 6 and 7). Based on detailed geologic mapping (**1**) the lower ~60% of borehole 56-29 probably did not penetrate the Harkless Formation, but instead encountered coarse, Esmeralda-Formation sedimentary breccia rich in Harkless clasts; (**2**) the *Taf* of the western part of section X-X' is interbedded with the Esmeralda and much less extensive than shown; and (**3**) the *Taf* of the eastern part actually occurs as small, isolated, and steeply-dipping sills or sublacustrine eruptives. If borehole 21-30 did in fact remain in *Taf* to total depth, then the hole probably peneterated a source vent for the ignimbrite.

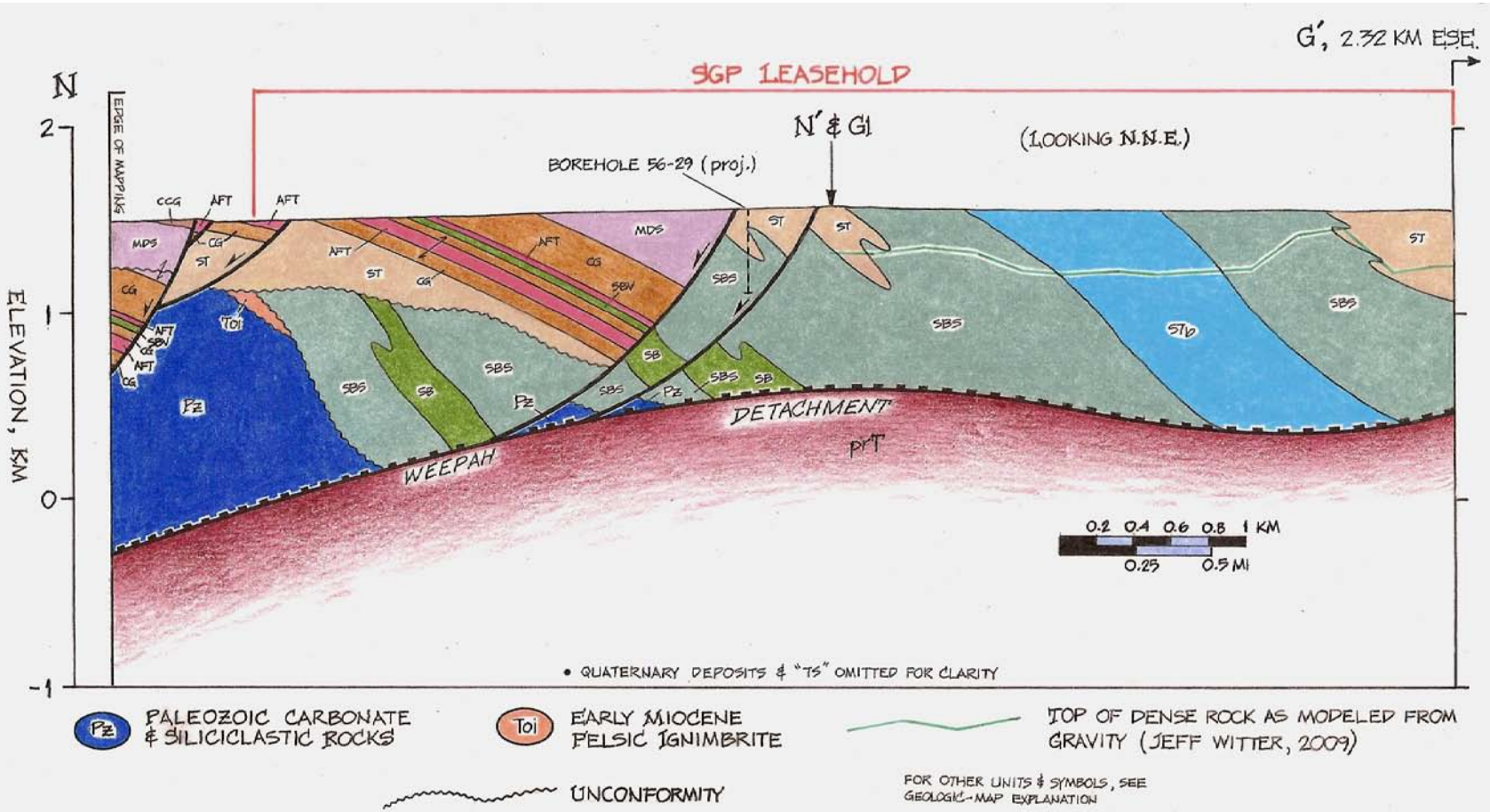

Figure 6. Interpretive geologic section **N-N'** and ~3/5 of **G1-G'** (see Figures 3 and 4 for location). The interpretation shown is considered by the writer to be the most plausible among several permissible within constraints provided by detailed geologic mapping, gravity modeling (G1-G' only; see also G-G1; Figure 7), and the regional geologic setting. The eastern half of the section is dominated by early, coarse clastic rocks—including massive landslide breccias—of the Miocene Esmeralda Formation. The coarse clastics were shed westward—from the initial headwall breakaway fault (since eroded away) of the Weepah detachment—into an inaugural supra-detachment basin of the Silver Peak-Lone Mountain metamorphic core complex (Figures 1 and 2). These early Esmeralda deposits were moderately to tightly folded and eroded prior to formation of a second supradetachment basin to the west. The second basin is bounded on its eastern edge by a major listric-fault-zone couplet that soles westward into the detachment. The detachment and these listric faults are envisioned to be the principal controls on modern thermal-fluid flow in the Alum geothermal prospect. ***Note***—the portrayed configuration and depth of the detachment are reasonable (based on westward projection from the structure's exposed trace to the east) but conjectural: The feature permissibly could be shallower or deeper and have greater or lesser relief than shown.

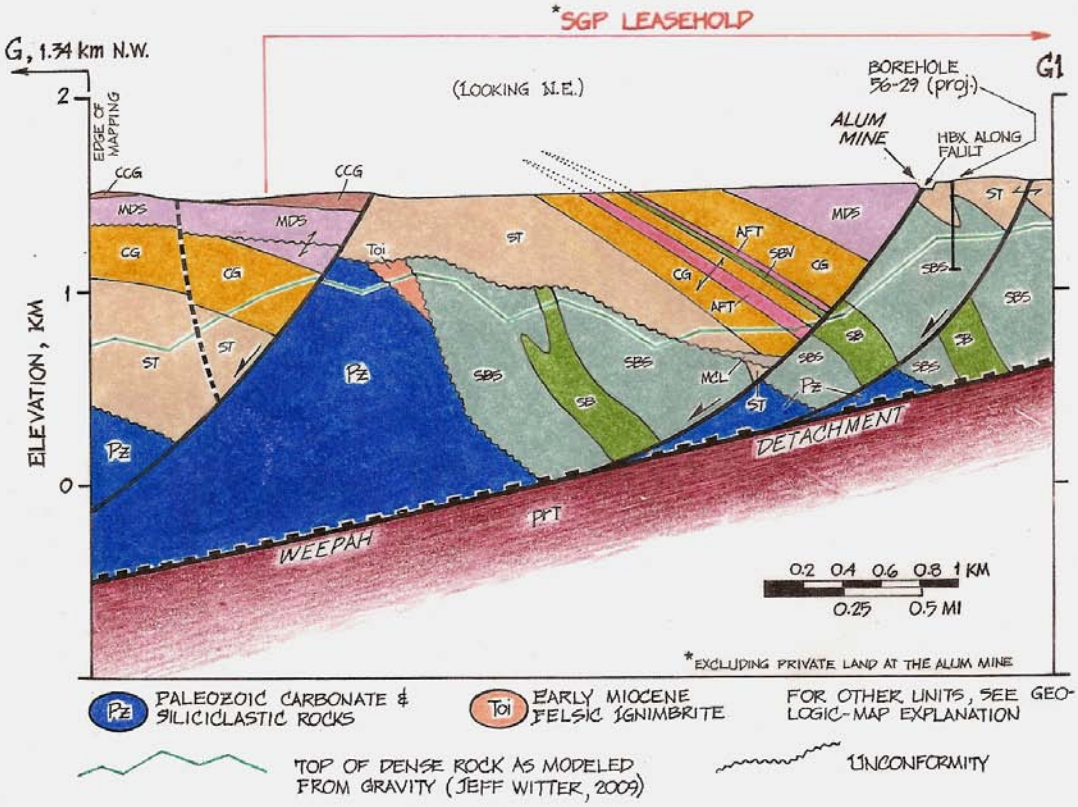

Figure 7. Interpretive geologic section along a portion of gravity-modeled depth-to-dense-rock profile **G-G1** (see Figures 3 and 4 for location; and Figure 6 for **G1-G'** southeastward extension of the section). Commentary essentially the same as for Figure 6. Alum-sulfur mneralization and accompanying advanced-argillic hydrothermal alteration at the Alum mine—clearly localized along the listric-fault couplet shown in the eastern part of this section—may or may not be genetically affiliated with spatially coincident modern geothermal activity (e.g., the boiling water and H_2S encountered in AMAX borehole 56-29).

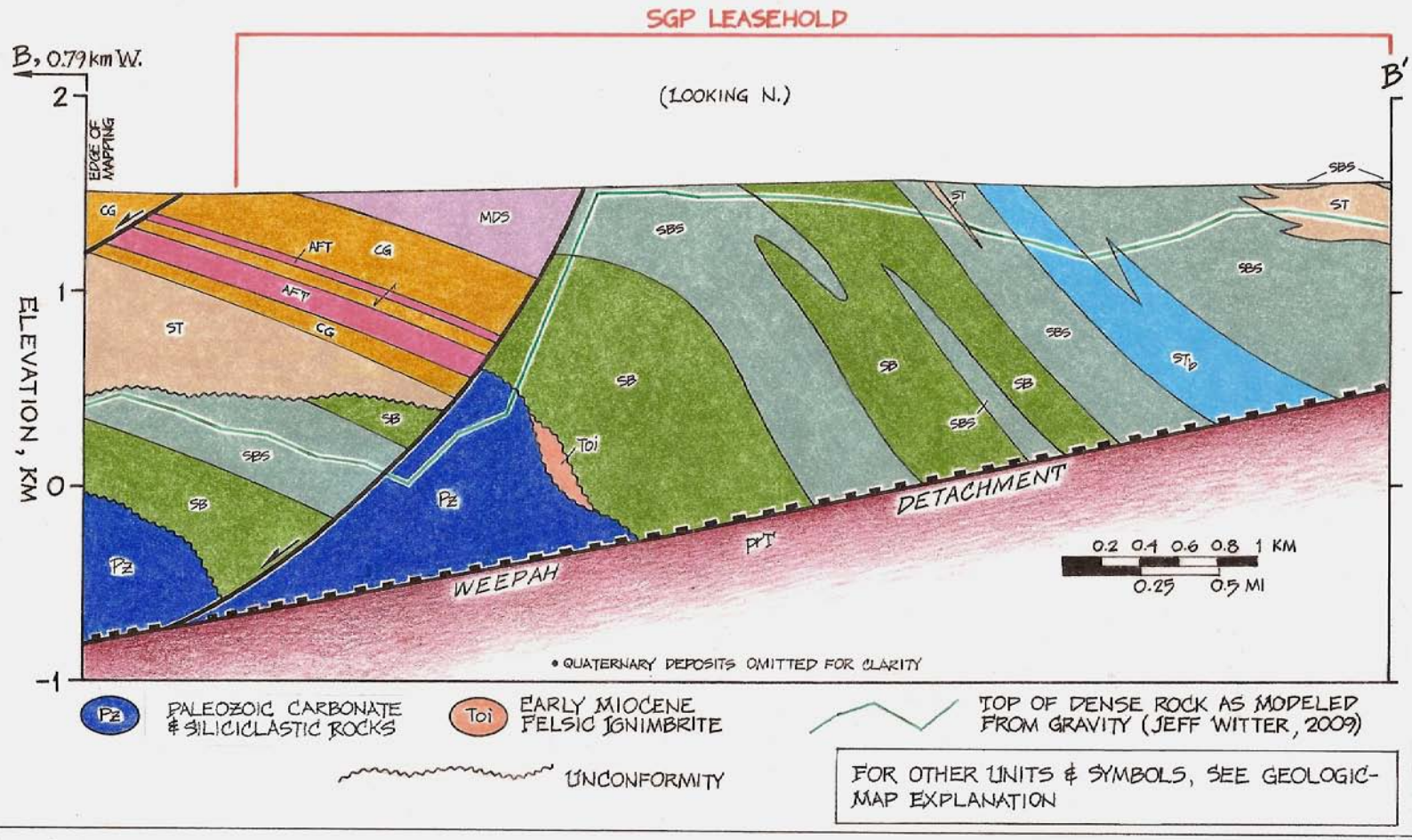

Figure 8. Interpretive geologic section along most of gravity-modeled, depth-to-dense-rock profile **B-B'** (see Figures 3 and 4 for location). Commentary essentially the same as for Figure 6. The top of the steep gravity scarp a little west of center on this section corresponds remarkably well with the surface trace of a mapped, major, down-to-the-west normal fault. Based on the gravity modeling, the throw of this fault on B-B' is greater than where the structure intersects the sections to the north (Figures 6 and 7).

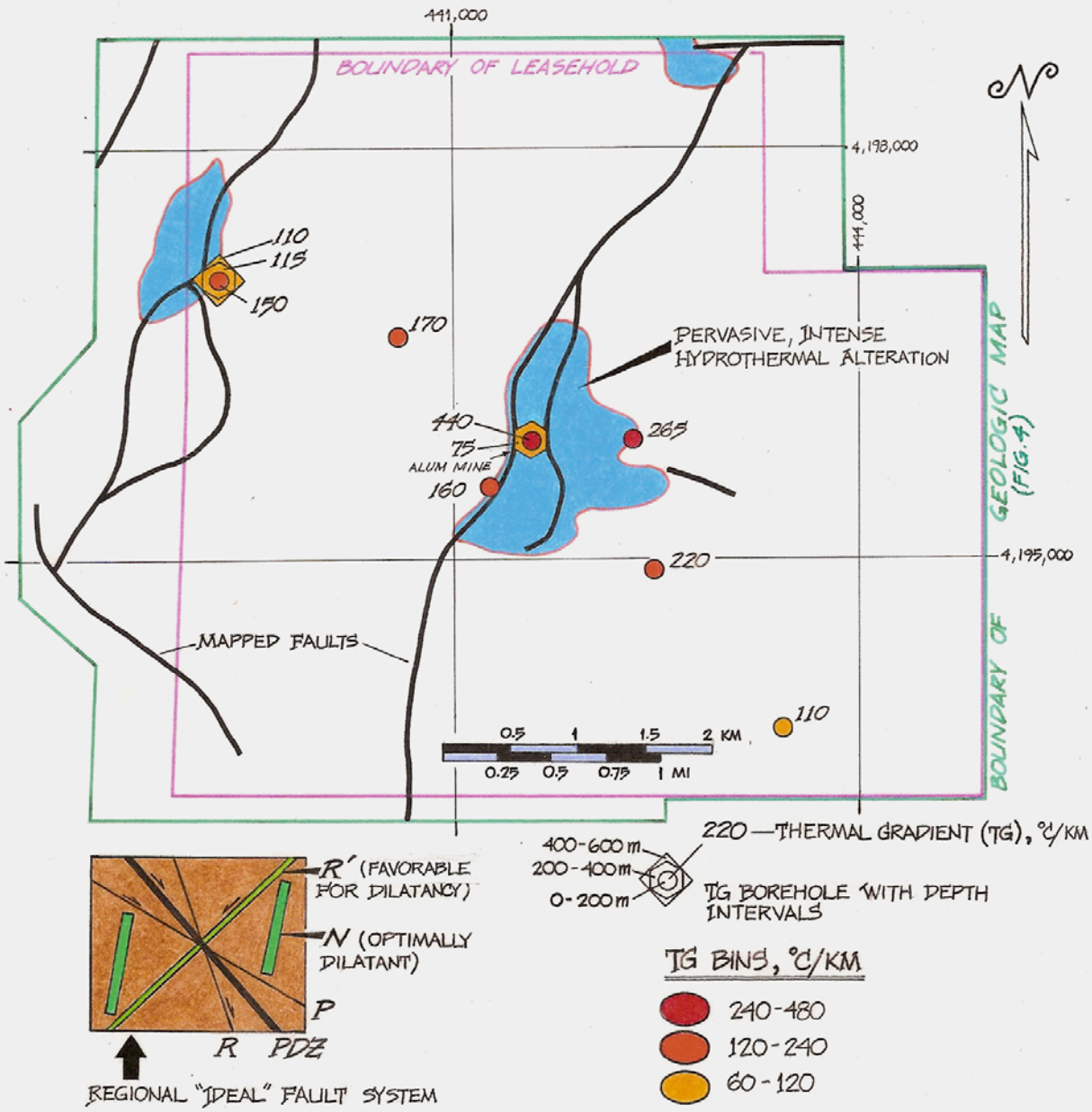

Figure 9. Mapped faults, hydrothermal alteration, and shallow (≥200 m to 600 m) thermal gradients in the Alum geothermal prospect. Shown for comparison are idealized fault trends and styles (light brown and green box at lower left) for this sector of the Walker Lane (see Figure 1). In this model, the right-lateral strike-slip principal displacement zone (**PDZ**) is oriented ~N40°W. Subsidiary strike-slip faults expected to form in this regime: **R**, or synthetic right-lateral shears; **R'**, or antithetic left-lateral shears; and right-lateral **P** shears. Corresponding, optimally permeable, normal-oblique (**N**) extensional faults are oriented north-northeast, subparallel to the Alum prospect's two major NNE-trending normal fault zones (including the one along which the Alum mine is located). Note that the prospect's three mapped intense-hydrothermal-alteration zones are also situated along these "**N**"-subparallel structures.

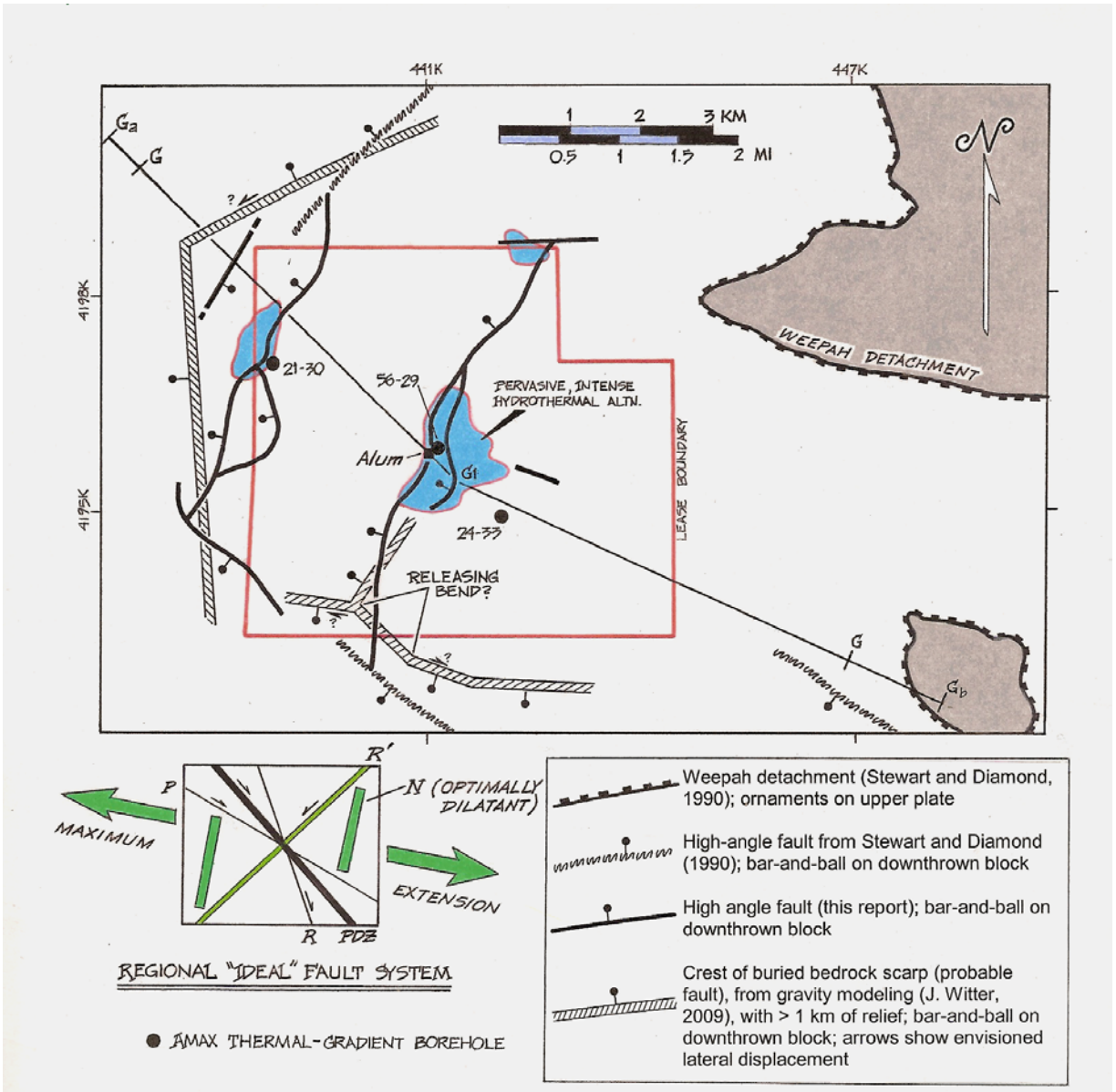

Figure 10. Generalized structure map of the Alum geothermal prospect and vicinity and western Weepah Hills, with the model "ideal" right-lateral wrench-fault system reproduced from Figure 9. Within this theoretical framework, the two major mapped, NNE-trending normal-oblique fault zones transecting the prospect should be optimally permeable, and therefore are likely to be key controls on the prospect's modern thermal-fluid upflow. Note, however, that the NNE-trending fault zones show little correspondence with the area's highest-relief (greater than 1 kilometer), gravity-modeled bedrock scarps. The northernmost and westernmost of these features—almost certainly faults themselves—are also conceptually viable permeability fairways, and may in fact be the principal sources (enabling "deep-circulation" heating) of the thermal fluids now circulating in the region. Another potential deeply-rooted, thermal-fluid-upflow "pipe" could be localized at a possible releasing bend along the southernmost gravity-modeled bedrock scarp/major fault.

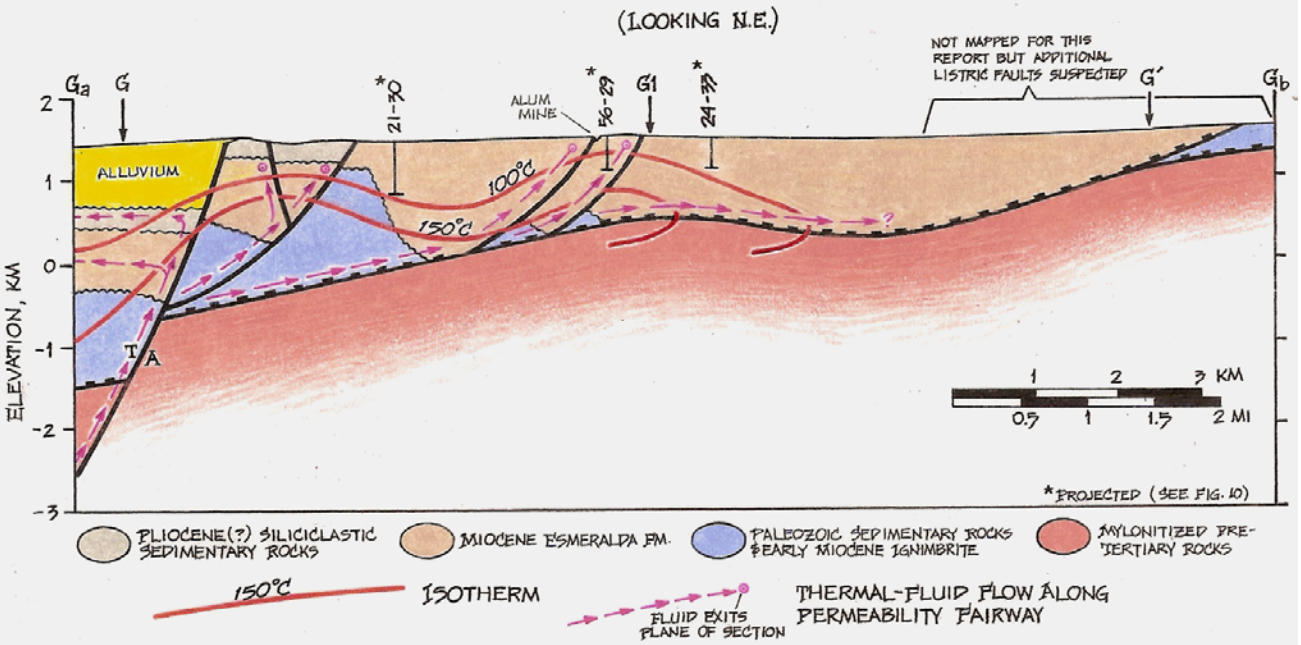

Figure 11. Conceptual model of the active Alum geothermal system, based on detailed geologic mapping, structural analysis, gravity modeling, very limited thermal-gradient (TG) drilling, and sparse geothermometry of hot waters retrieved from the TG boreholes. According to the model, thermal fluids heated by deep circulation ascend into the prospect area via a major, steeply-dipping, left-lateral-oblique fault zone at the southern margin of Big Smoky Valley basin (Figure 2). Some of the heated fluids advect back out into the basin at shallower elevations along permeable sandstone and conglomerate horizons in the Mio-Pliocene siliciclastic sequence that includes the Esmeralda Formation. The bulk of thermal-fluid advection, however, is deflected southeastward along the Weepah detachment of the Silver Peak-Lone Mountain metamorphic core complex (MCC); as well as upward along optimally configured listric faults in the MCC's upper plate. In essence, the existing TG boreholes tap a relatively high-temperature geothermal outflow plume.

The model shown is a conservative one, and changing one or more of three key variables could increase the envisioned reservoir depth range, volume, and temperature: (**1**) The heat source beneath the Alum mine conceivably could be plutonic, and genetically related there to hydrothermal brecciation, natural hydraulic fracturing, alum-sulfur mineralization, and associated advanced argillic alteration; (**2**) The Weepah detachment could be deeper than portrayed, allowing scope for higher temperatures with the greater depths; and more deeply-penetrating listric fault zones with attendant, higher-volume fracture networks; (**3**) The "listric" fault zones could also be "domino-style" block faults, with greater structural disruption and complexity where the blocks approach and contact the detachment. In the writer's opinion, item (1) is unlikely; but (2) and (3) are decidedly reasonable alternatives. Note also that thermal-fluid inflow could equally likely be entering the prospect from a major high-angle fault to the southwest (Figure 10). Please see text for additional explanation.

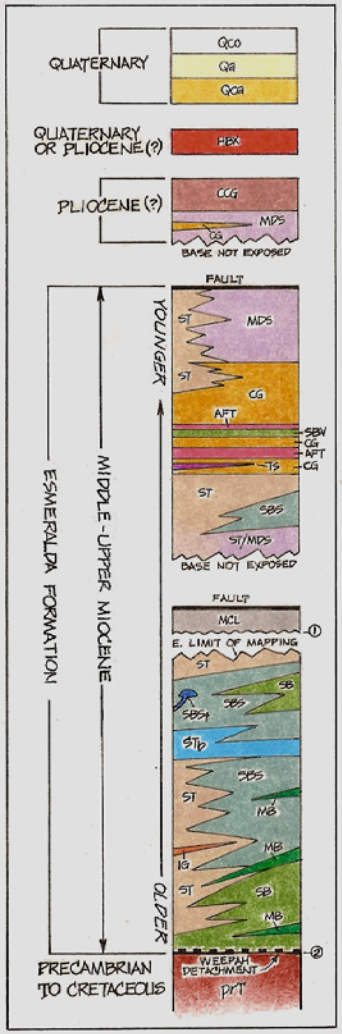

Qco—Rock obscured or concealed by cultural debris (e.g., fill material; mine dumps).

Qa—Alluvium

Qoa—Older alluvium

HBX—Hydrothermal breccia—Dilational breccia with angular wallrock clasts, up to 1 meter in diameter, in a matrix variably of rock flour and open-space-filling minerals.

CCG—Coarse conglomerate. Pebble- to small-boulder (typically cobble) conglomerate, poorly sorted, matrix- to clast-supported. Commonly weakly consolidated.

MDS—Dominantly whitish tuffaceous mudstone, planar-laminated, with minor local sandstone to pebble conglomerate [**CG**; see below]. Commonly gypsiferous and smectite-altered, with a "popcorn" weathering texture. Probably of lacustrine origin.

ST—Dominantly siltstone to fine-grained sandstone, planar to low-angle cross-laminated, platy-weathering, with minor local tuffaceous mudstone and coarser siliciclastics.

CG—Interstratified pebble conglomerate and sandstone.

AFT—Felsic, vitric-lithic ash-flow tuff. Stewart and Diamond's (1990) tuff of Big Smoky Valley.

SBV—Felsic-volcanic-clast sedimentary breccia. Isolated boulders up to 5 meters in diameter.

TS—Muddy to silty felsic fallout tuff, whitish, locally opalized.

MCL—Mixed sedimentary breccia, conglomerate, sandstone, and tuffaceous mudstone.

SB—Coarse sedimentary breccia. Massive, unsorted aggregate of angular clasts of Paleozoic siliciclastic and carbonate rocks, with minor Tertiary volcanics, embedded in a rock-flour matrix of the same composition. Clasts range in size from pebbles to boulders up to 5 meters in diameter. Unit has a grayish-green cast due to decomposition of chloritic siliciclastics. Landslide and debris-flow deposits.

SBS—Similar to "**SB**," but locally crudely stratified and better sorted, as well as interstratified with medium- to coarse-grained sandstone and pebble to cobble conglomerate.

SBSt—As above, but extensively veined and possibly interstratified with travertine.

STb—Whitish tuffaceous mudstone and siltstone (minor local sandstone) interstratified with thin beds of "**SB**" (see above). Includes abundant small mounds and stringers of thinolitic tufa.

IG—Felsic vitric ignimbrite, non-welded but densely silicified. Sills or sublacustrine eruptives.

MB—Megabreccia. Same texture and composition as "**SB**" (see above), but with clasts up to at least 75 meters in diameter. Catastrophic-landslide deposits.

prT—Mylonitized Precambrian through Cretaceous rocks, undivided. Lower plate of the Weepah (Silver Peak-Lone Mountain) metamorphic core complex. Cross sections only

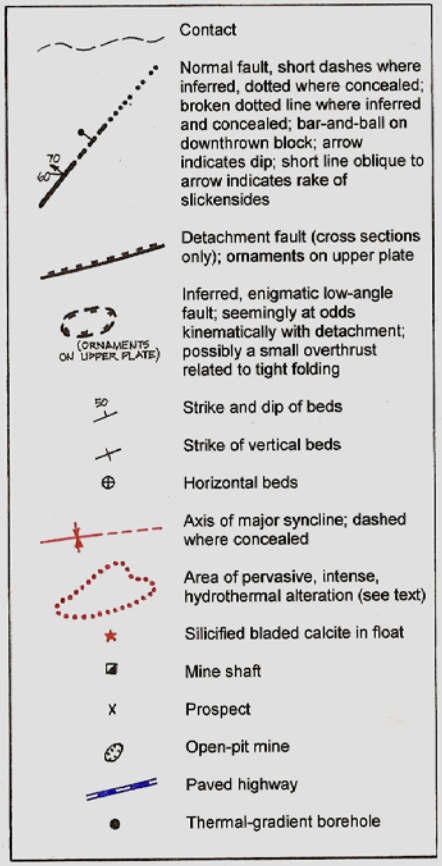

EXPLANATION FOR SIMPLIFIED GEOLOGIC MAP OF THE ALUM PROSPECT, ESMERALDA COUNTY, NEVADA

Jeffrey B. Hulen June 2009